



**Michigan
Technological
University**

Michigan Technological University
Digital Commons @ Michigan Tech

Dissertations, Master's Theses and Master's Reports

2021

APPLICATION OF REMOTE SENSING FOR PERMAFROST MONITORING IN ALASKA

Iuliia V. Tcibulnikova

Michigan Technological University, itcibuln@mtu.edu

Copyright 2021 Iuliia V. Tcibulnikova

Recommended Citation

Tcibulnikova, Iuliia V., "APPLICATION OF REMOTE SENSING FOR PERMAFROST MONITORING IN ALASKA", Open Access Master's Thesis, Michigan Technological University, 2021.
<https://doi.org/10.37099/mtu.dc.etr/1192>

Follow this and additional works at: <https://digitalcommons.mtu.edu/etr>



Part of the [Geological Engineering Commons](#)

APPLICATION OF REMOTE SENSING FOR PERMAFROST MONITORING IN
ALASKA

By

Iuliia V. Tcibulnikova

A THESIS

Submitted in partial fulfillment of the requirements for the degree of

MASTER OF SCIENCE

In Geological Engineering

MICHIGAN TECHNOLOGICAL UNIVERSITY

2021

© 2021 Iuliia V. Tcibulnikova

This thesis has been approved in partial fulfillment of the requirements for the Degree of MASTER OF SCIENCE in Geological Engineering.

Department of Geological and Mining Engineering and Sciences

Thesis Advisor: *Thomas Oommen*

Committee Member: *Kenneth Hinkel*

Committee Member: *Stanley Vitton*

Department Chair: *Alexey Smirnov*

Table of Contents

List of Figures	4
List of Tables	6
Acknowledgements.....	7
Abstract.....	8
1 Introduction	9
1.1 Aims and objectives.....	9
1.2 Motivation for research.....	9
2 Literature Review	12
2.1 Permafrost.....	12
2.2 The Arctic	15
2.3 Thaw lakes.....	17
3 Study area.....	21
4 Methodology	26
4.1 Normalized Difference Water Index.....	27
4.2 Lake Depiction.....	29
5 Results	30
5.1 Lake Growth Rate	34
5.2 Examples of lakes	50
6 Discussion	59
6.1 Ground ice content.....	59
6.2 Influence of infrastructure.....	61
6.3 Precipitation	63
7 Conclusion.....	64
8 Reference List.....	66

List of Figures

Figure 1 Projected rate of change per year of industry activities and the physical environment up to 2050: Sea ice (-1.2%), Tourism (24.9%), Shipping (6.4%), Fishing (0.4%), Oil production (0.6%), and Mining (1.1%), (Williams et al., 2011).	10
Figure 2. Profile of permafrost; undisturbed is to the right; disturbed by human interaction is to the left (Mackay, 1992).	14
Figure 3 Distribution of permafrost in the Arctic (Brown et al, 2002).	16
Figure 4. Oriented thaw lakes in Alaska (Black, Barksdale, 1949).	18
Figure 5. Development of a thaw lake, Alaska. (Jones, Arp, 2009)	20
Figure 6. Study area location within Alaska.	22
Figure 7. Digital elevation model of the area (DEM courtesy of the U.S. Geological Survey).	25
Figure 8. Combined map of NDWI values of 2020 (dry land) and 2013 (open water).	29
Figure 9. Histogram showing the distribution of lake area.	31
Figure 10. Spatial distribution of lake size according to Table 1 (year 2020).	34
Figure 11. Spatial distribution of the thaw lakes by growth rate by 2020.	36
Figure 12. Histogram of lake area change rate in percent.	36
Figure 13. Verifying the area assessment for lake 1 (2013 area is the outline, 2020 area is filled)	37
Figure 14. Verifying the area assessment for lake 2 (2013 area is the outline, 2020 area is filled)	38
Figure 15. Verifying the area assessment for lake 3 (2013 area is the outline, 2020 area is filled)	39
Figure 16. Scatter plot of lake area change in pixels.	41
Figure 17. Merging of small lakes with a large one.	43
Figure 18. Merging of small lakes with a larger one.	45
Figure 19. Lakes over 5000 m ² and their change in pixels below 100.	47
Figure 20. Histogram of area change in pixels.	47
Figure 21. Difference in cell count versus the lake area (m ²).	48
Figure 22. Merging of two lakes over 0.5 ha.	49
Figure 23. Example of a moderately grown lake; A – 2013, B – 2020, C – high resolution 2020.	51

Figure 24. Example of a moderately grown lake; A – 2013, B – 2020, C – high resolution 2020.....	53
Figure 25. Example of a moderately grown lake; A – 2013, B – 2020, C – high resolution 2020.....	55
Figure 26. Example of a significantly shrunk lake; A – 2013, B – 2020, C – high resolution 2020.....	56
Figure 27. Example of a significantly grown lake; A – 2013, B – 2020, C – high resolution 2020.....	58
Figure 28. Permafrost types in the study area (data sourced from Brown et al, 2002).....	60
Figure 29. Roads in the study area (data sourced from State of Alaska Open Geodata Portal, 2019).....	63

List of Tables

Table 1. Lake area statistics	31
Table 2. Checking the assessment of sample lakes.....	40

Acknowledgements

I would like to first thank the United States Department of State and their Fulbright Foreign Student Program for giving me this amazing opportunity to advance my education and broaden my horizons.

give my heartfelt thanks to my academic advisor, Dr. Thomas Oommen, for giving me the necessary guidance throughout working on this thesis. Your honest feedback had pushed me to discover new perspectives in my research.

I would also like to thank Dr. Kenneth Hinkel for his incredibly valuable insights on the methodology, and Dr. Stanley Vitton for his advice on the thesis outline.

In addition, I would like to thank my Mom and Dad for believing in me in the process!

Abstract

Permafrost covers about 85% of the state of Alaska; it is a fragile cryogenic phenomenon prone to degradation under thermal and mechanical (natural and anthropogenic) influences. This research analyzes the application of remote sensing for permafrost monitoring in the Prudhoe Bay area, Alaska. Thawing thermokarst lakes are assessed as the signs of permafrost degradation. Normalized Difference Water Index (NDWI) was used to detect thaw lakes in Landsat-8 satellite imagery within the 529-km² study area in 2013 and 2020. The lakes were then mapped according to their size and growth rate. Lakes do not grow uniformly; some lakes grow while other lakes decrease in size. Very small lakes are found to have higher growth rates; they are shallower, so their area rapidly increases with influx of precipitation. Lakes have been observed to merge together, Lakes are less abundant in the south-western part of the study area, where the ground surface elevation increases and ground ice content decreases from high to low. The network of roads in the study area was determined to affect the distribution of lakes. The cumulative area of thaw lakes has increased over the study period, however, the number of lakes has decreased, Factors affecting the spatial distribution of lakes were assessed, such as the ground ice content and cumulative precipitation. The NDWI method has proven itself useful for open water and wetland detection in the tundra plains setting. Limitations of the method's application were determined.

1 Introduction

Thawing of permafrost is dangerous in polar regions because it destroys the disrupts ecosystems and destroys man-made structures. For industrial activities in the Arctic, among which is petroleum engineering, stable ground is the key factor in territorial planning. Permafrost monitoring is challenging due to the remoteness of the region and harsh climatic conditions. Nevertheless, scientists and industrial specialists find ways of keeping track of permafrost dynamics.

Remote sensing is useful for global-scale assessment because it provides access to data for areas that may be otherwise inaccessible. Remote sensing is applied for such purposes as:

- Detecting sites where permafrost changes are occurring most rapidly, thus pointing at crucial sites for investigating.
- Modeling of subsurface permafrost;
- Supporting existing in situ measurements by providing timely area coverage (obtaining data for a site when fieldwork is over);
- Extrapolating field data onto more expansive areas.

1.1 Aims and objectives.

This research **aims** to determine the trends in the development of permafrost in the Prudhoe Bay area, Alaska. The **objectives** that help achieve this goal are as follows:

- Detection of secondary signs of permafrost degradation in the form of thaw lakes using remote sensing images within the study area.
- Assessment of temporal rate of change in surface area of said thaw lakes;
- Discussion of results to determine the factors affecting the formation and development of the thaw lakes within the study area.

1.2 Motivation for research

The motivation for this research comes from the realization that the human presence in the Arctic is inevitable, according to contemporary forecasts on global sustainable development (IISD, 2019). According to Williams et al. (2011), by the year 2050, the growth of the industry in the Arctic is projected to reach anywhere between 1% for oil, gas, mining, and 24% for tourism (difference in percent from year 2000) (see Fig. 1). The

average annual extent of sea ice is, however, predicted to decrease by 1.2%. While that directly means the increase in maritime navigation across the Arctic ocean, it also promotes industrial development onshore. To ensure sustainable development of the Arctic, intensive research and monitoring of environmental conditions under human influence is extremely important.

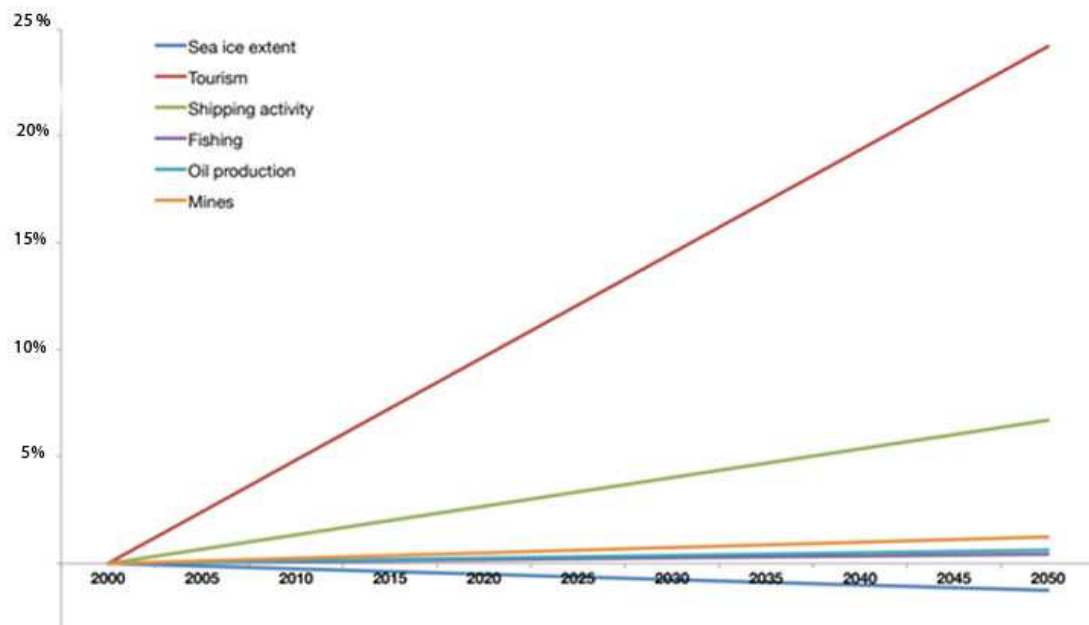


Figure 1 Projected rate of change per year of industry activities and the physical environment up to 2050: Sea ice (-1.2%), Tourism (24.9%), Shipping (6.4%), Fishing (0.4%), Oil production (0.6%), and Mining (1.1%), (Williams et al., 2011).

The importance of using remote sensing for assessment of issues associated with industrial expansion is evident. Thermokarst lakes and their drained basins at the North Slope of Alaska vary in size for a vast range and can be as small as 30 meters in length, which cannot be seen on typical topographic maps of the region (Frohn et al., 2005).

The Arctic is known for its cold and hostile environment (U.N. Environment. n.d). For most people working there, the bare flattened landscape of the Arctic tundra is unusual, which, together with remoteness from centers of civilization, 'can lead to unpleasant health consequences.

The remoteness of the region makes it difficult to deliver and administer food supplies and medical care. The Arctic is one of the most sparsely populated regions in the world (Arctic.ru n.d.; Young et al., 2010); which complicates the communication between think tanks "on land" and research expeditions in the field. The Arctic is also divided into

sectors between eight countries. The countries of the Arctic Council (including the United States of America, the Russian Federation, and Denmark) are making efforts to cooperate on the research and preservation of the Arctic. However, issues in international relations might complicate international field trips to the circumpolar areas.

Since Arctic biota is precisely fit for an extreme but narrow range of temperatures, the proper functioning of circumpolar biomes depends on particular, very cold, climatic conditions. As the foundation for 70% of the Arctic, permafrost is dependant on continuous low temperatures (Karjalainen et al., 2019). Permafrost on dry land can be defined as soil or bedrock at or below 0 °C for two or more consecutive years. It is a natural phenomenon formed because of peculiar thermal dynamics in the high latitudes.

From the point of view of infrastructure engineering, frozen soils underlay the foundations of constructions; therefore, if permafrost under a building is damaged, the building itself may get damaged from the differential settlement in its foundation (Okhlopko, 2018). The lateral extent of permafrost and its latitudinal distribution to the south may decrease substantially by the end of the XXI century. However, the magnitude of change is mostly by local factors (now, vegetation, soil texture and moisture, solar radiation, and surface hydrology) (Karjalainen et al., 2019).

Since the 1940's, the international scientific and engineering community has been researching the phenomenon of permafrost and developing effective and sustainable practices of permafrost engineering. The International Permafrost Association (IPA) organizes frequent conferences, where specialists from all over the world have the opportunity to communicate efficiently (Schollaen et al, 2014). Great international attention to the problems of the Arctic has motivated me to conduct this research and contribute to the advancement of permafrost engineering.

2 Literature Review

Not only does the Arctic warm up twice as fast as the rest of the planet (Post et al, 2019), but circumpolar landscapes are more vulnerable to the changes in the environment (Jorgenson, Grosse, 2016). The Arctic undergoes a constant shift of permafrost-covered zones towards the north (Kääb, 2008). It is predicted that more than 40% of permafrost-covered land will be free of it by the year 2100, according to Wagner et al. (2018). At the same time, human activities (petroleum exploration, tourism, non-indigenous settlements, etc.) will also expand in higher latitudes, thus affecting the permafrost.

2.1 Permafrost

The ACP is covered predominantly by tundra, a type of terrain is characterized by low-lying vegetation and low plant growth rate (Osborne et al., 2018). According to Brown et al. (2002), the region is underlain mainly by continuous permafrost. Sedimentary deposits and the bedrock to a depth of several hundred meters under the High Arctic are permanently frozen. The upper layer of permafrost on the major part of the Northern Slope of Alaska contains vast amounts of ice in the form of "nearly vertical ice wedges, horizontal ice sheets, irregular ice masses, and small grains, crystals, stringers, irregular particles, and films of ice as a cement." Shallow thaw zones called taliks occur under water-bodies, for the temperature of liquid water is warmer than the surrounding ice, and it transfers heat to the lake sediments.

The active layer of permafrost is the upper layer that typically thaws in summer and refreezes in winter (Dobinski, 2020). The average thickness of the thawed active layer in summer is about 8-20 inches. (Black, Barksdale, 1949).

The hydrographic network of surface water is affected by the permafrost: water exchange and flow are frequently interrupted by annual freeze-thaw cycles. Because of impermeable layers of the frozen ground below, surface waters cannot drain, hence the great abundance of wetlands throughout the Arctic tundra (Belikovich, 2001; Hinkel et al., 2005). Significant amounts of water are retained in the Alaskan tundra, forming vast wetlands. The main factors for retaining water are low summer temperature and evaporation due to the short summer season (only three to four months from July to October), long frozen periods (the rest of the year). The mean date of full ice clearing is the 1st of June, of lake freeze-over is the 1st of October.

Studies show a negative impact on the condition of permafrost from vehicle traffic, camp construction, and drilling activities, and the effects are more substantial in areas with ice-rich soils, however, most of the impact comes from building heated structures atop of the

permafrost. For example, trails from vehicles used during petroleum exploration in the 1950s are still visible in satellite imagery (Hinkel et al., 2017).

Permafrost is recognized as the "essential climate variable" by the World Meteorological Organization. There are global initiatives about permafrost monitoring, such as the "Circumpolar Active Layer Monitoring" (CALM) and the "Thermal State of Permafrost" (TSP), curated by international environmental agencies (Bartsch, 2014). They are working towards creating a global map of permafrost conditions. Apart from geotechnical issues for the infrastructure, thawing permafrost also poses a threat to the atmosphere. The Arctic tundra and its permafrost are some of the world's most significant carbon reservoirs. This reservoir is extremely temperature-sensitive: as the depth of the active layer or the seasonal thaw layer thickens in response to the rising temperatures in the Arctic, enhanced microbial activity in the thawed soil would transfer the soil organic carbon into the atmosphere in the forms of methane and carbon dioxide (Schuur, 2019; Frohn et al., 2005).

Additionally, permafrost can facilitate the formation of gas hydrates, which, when uncovered after the permafrost melts, release methane (also a GHG) into the atmosphere. Therefore, permafrost protects the planet from overheating by storing potential GHGs. Permafrost, as the cryogenic phenomenon, is protected in the United States at the government level: most traffic has been restricted to specific routes and is permitted to travel only in winter-time (Hinkel et al., 2017).

In Figure 2, we can see the profile of permafrost. In the left part of the picture, permafrost is undisturbed. Therefore, the active layer is within its natural thickness of 50 cm. If the upper turf layer and part of the active layer are removed by humans, the active layer thaws much deeper and gains a thawed thickness of 100 cm. When permafrost thaws, the excess ice inside it turns to water, and the whole mass subsides. In figure 2, there is dramatic subsidence of ground in the right part of the figure.

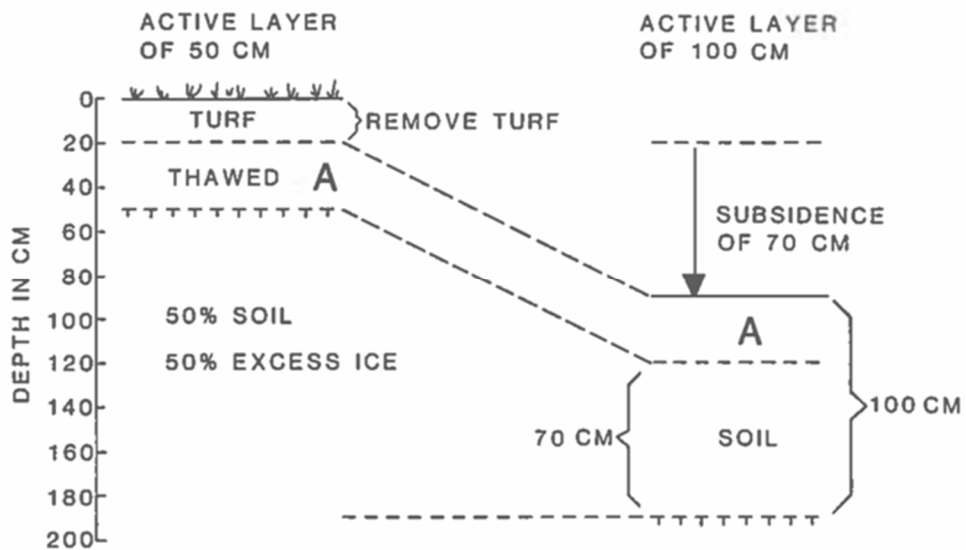


Figure 2. Profile of permafrost; undisturbed is to the right; disturbed by human interaction is to the left (Mackay, 1992).

2.1.1 Climate change and permafrost degradation

In Alaska, climate change affects permafrost. For example, the rates of coastal erosion along the coast of the Beaufort Sea have more than doubled over the past fifty years. An average rate of $0.48 \text{ km}^2/\text{yr}^{-1}$ during 1955–1985 to $1.08 \text{ km}^2/\text{yr}^{-1}$ during 1985–2005 has been computed using the information from analyzing topographic maps and satellite images (Mars, Houseknecht, 2007).

Proposed climate change effects for the High Arctic include:

- Thickening of the active layer;
- Increase in precipitation;
- Thaw subsidence where permafrost is ice-rich;
- Increased snowfall, which would lead to lake levels rising and drainage through overtopping;
- The occurrence of new small thermokarst lakes;
- Termination of development of old thermokarst lakes (because the ice-rich permafrost has already thawed).

Infrastructure engineering in the higher latitudes leads to the thawing of both continuous and discontinuous permafrost, which destroys the terrain even when there is no climate change (Hughes, n.d.). Constantly heated constructions inevitably transfer heat into the underlying ice-rich upper layer of the permafrost. This effect has been observed by engineers all across the Arctic.

Geomorphological changes mainly occur under the influence of topography, which is also important for the components of solar energy absorption and reflection. All of this is affecting permafrost, indeed. Thus, research in remote sensing applications for engineering in the Arctic currently is focused on 'identifying quantitative relationships between topography, geomorphological processes, and energy distribution within a distributed modeling framework' (Etzelmüller et al., 2001).

There are a number of natural processes that can be claimed to be stemming from, or caused by, permafrost. Whether it is growing, degrading, or stable, permafrost creates specific conditions that completely change the way of engineering on the site (Malneva, 2016). Traditional methods of assessing the soil and the following foundation design are often not valid in the circumpolar regions. Geological engineers in the Arctic have to

consider the various permafrost-related processes that are common for the higher latitudes. These processes can be grouped into the following categories (Kääb, 2008).:

- Floods resulting from massive thawing of ice-rich permafrost, dissolving banks of water bodies;
- Mass movement, which occurs when ice bonding the ground melts, and the ground collapses; ground subsidence and thaw can be categorized as mass movement events, as well as slope creep and instability.
- Thaw-frost heave, when ice wedges form, and solid monoliths of soil acquire cracks that lower their bearing capacity;
- Ground subsidence - rapid vertical movement of the ground surface in circumpolar areas occurring due to the thawing of underlying permafrost (Wagner et al., 2018).
- Surface water drainage that affects indigenous populations through disturbing freshwater supply (Bartsch, 2014).

2.2 The Arctic

The Arctic is the northernmost region of the planet Earth, located in the Northern hemisphere around the North pole. The southern limit of the region is the southern extent of the tundra, the natural zone characterized by hindered tree growth due to cold climates and permafrost. Tree roots cannot penetrate the frozen ground, so large trees do not grow in the tundra; the typical flat plain landscape is covered with shrubs, grasses, sedges, mosses and dwarf trees (NSIDC, 2020). The Arctic is also frequently delimited as the lands above the Polar Circle, the hypothetical line on the surface of the planet, above which the polar night and day phenomena are observable (Cessna, 2009).

24% of the Northern Hemisphere is covered by permafrost; most of it located in the Arctic (NSIDC, 2017). Figure 3 depicts the distribution of types of permafrost around the Arctic. Permafrost is divided into four types: continuous, discontinuous, sporadic and isolated. Continuous permafrost exists as an uninterrupted layer, whereas the following types of permafrost are characterized by separation in permafrost locations (Donev, 2016).



Figure 3 Distribution of permafrost in the Arctic (Brown et al, 2002).

2.2.1 Climate

The climate on the Arctic slope is cloudy, cold, arid, and windy. According to the data from the National Centers for Environmental Information (NOAA.gov, 2011), the mean annual temperature at the measuring station closest to this research's study area (the Deadhorse Airport, AK), is 11.5 °F (-11 °C), mean winter temperature is -14.7 °F (-25 °C), and mean summer temperature is 42 °F (5.5 °C). The current absolute maximum temperature is 100 °F (38 °C). and the absolute minimum temperature is -

80°F (-62°C) (Sulikowska et al., 2019). Average annual rainfall reaches 10 cm, whereas the snowfall is 60 cm; the prevailing wind direction throughout the year is the east, with speeds varying from 20 km/h in winter to 15 km/h in summer (Weatherspark.com, 2021).

The temperature of the air in the Arctic has been steadily rising for the past couple of decades. The mean global temperature to the north of 60°N has increased to 2 °C since the late 1960s. The Arctic is warming faster in winter and spring and the smallest in fall. Measurements in drilling holes suggest that the permafrost temperatures have been increasing during the last 50 years with higher than mean rates of warming in Alaska, Canada, Scandinavia, and Russia (Lecavalier et al., 2017). There is evidence that natural disturbances in the Arctic are becoming more frequent and devastating, attributed to two main factors - human interaction and global climate change (Lantz, 2017). For example, more and more wildfires in the Arctic tundra occur from lightning strikes (Waldman, 2017). Extreme thermal regimes affect the distribution of liquid water: most available water is in a frozen state of ice and snow, making it very energy-intensive to melt the ice and obtain fresh water.

2.2.2 The Arctic Coastal Plain

The Arctic Coastal Plain (ACP) is the northernmost region of Alaska and northwestern Canada. The landscape there is relatively low and flat, with elevations barely reaching 100 m (Hinkel et al., 2005, 2007). This geomorphological province is located to the north from the Brooks range, and has the Arctic Ocean in the north. The south limit of the province is the Arctic Foothills, the northern piedmont of the Brooks Range. From the geological point of view, the territory of the ACP is underlain by “ice-bonded Quaternary marine, fluvial and aeolian sediments atop slightly dipping Cretaceous sedimentary rock” (Hinkel et al., 2005). Multiple marine transgressions can be observed in the sediments from the late Cenozoic; the presence of ancient shorelines across the region supports this notion. The ACP has been tectonically stable for at least the last 125 kyr (Hinkel et al., 2005).

2.3 Thaw lakes.

A prominent characteristic of The North Slope of Alaska is the abundance of thaw lakes (also called thermokarst lakes) and drained lake basins developed within the distribution of continuous permafrost. Thaw lakes might be the most significant feature of the tundra landscape. There are tens of thousands of them across the ACP (Hinkel et al., 2005).

Since the surface-level moisture content is high in the Arctic tundra, lakes often form in depressions. It has been estimated that from 50% to 75% of the ACP is covered with thaw lakes and drained lake basins spread across tundra wetland (Black, Barksdale, 1949; (Frohn et al., 2005)).

Most of the thaw lakes are elliptical and oriented with the long axis of the elliptical lake at 10°–20° west of geographic north and nearly perpendicular to the prevailing easterly wind direction (see Fig. 4). This alignment is so prominent that it was used in aircraft navigation. Figure 4 is an aerial photograph of oriented thaw lakes in Alaska. Erosion of banks when the lake is clear of ice occurs perpendicularly to the direction of prevailing winds, resulting from specific wave action. Slow bottom subsidence of lake basins is due to the lack of thawable massive ice in deeper layers of permafrost (Brewer, 1958).



Figure 4. Oriented thaw lakes in Alaska (Black, Barksdale, 1949).

The main areas of erosion in a lake basin are in the upper layer of permafrost, where it contains up to 50% of ice by volume (Mackay, 1992).

Usually, the lakes have relatively smooth shorelines, mostly in lowland areas, and have elongated shapes. The majority of the lakes at the ACP are less than 2 m deep (Hinkel, 2006). Some lakes form a shallow shelf and a deeper center, while some do not (Black, Barksdale, 1949). Thaw lakes sustain the local biodiversity. They provide fresh water and habitat to a variety of local species. The lakes are also considered an important water source for the indigenous communities and the industry (Jones et al., 2009).

Thaw lakes in the Arctic Coastal Plain develop according to a cycle: they grow and then disappear. The formation of some lakes begins on the surface, when small ponds develop at intersections of ice wedges or in low-center ice-wedge polygons. Together with the melting of permafrost under the movement of liquid water, thermal erosion along the shores enlarges these lakes. Thaw subsidence and thaw occur in the ice-rich upper layer of permafrost, and the basin becomes a reservoir for surface water runoff. When water depth exceeds about 2 m, lakes no longer freeze to their bottoms, and a talik forms beneath the lake basin. In more shallow basins (depth below 2 m), a talik does not develop because the winter ice cover freezes to the lake bottom. As the lake expands in size, smaller ponds and lakes around may be swallowed by it.

Drainage of the lake may be triggered by ice-wedge erosion, stream erosion, tapping, bank overflow, or coastal erosion. Most lakes drain partially, leaving residual ponds nested within the basin. After the lake drainage, vegetation covers new dry areas, filling the basin with organic material. Ice formation in permafrost is resumed. Ice wedge growth eventually forms polygonal terrain with new small ponds in depressions, and a new phase of the thaw lake cycle begins (Black et al., 1949). Figure 5 demonstrates how two thaw lakes merge; additional territory is being filled with water around the lakes as well. The mode of development of a lake is based on the stage of the thaw-lake cycle.

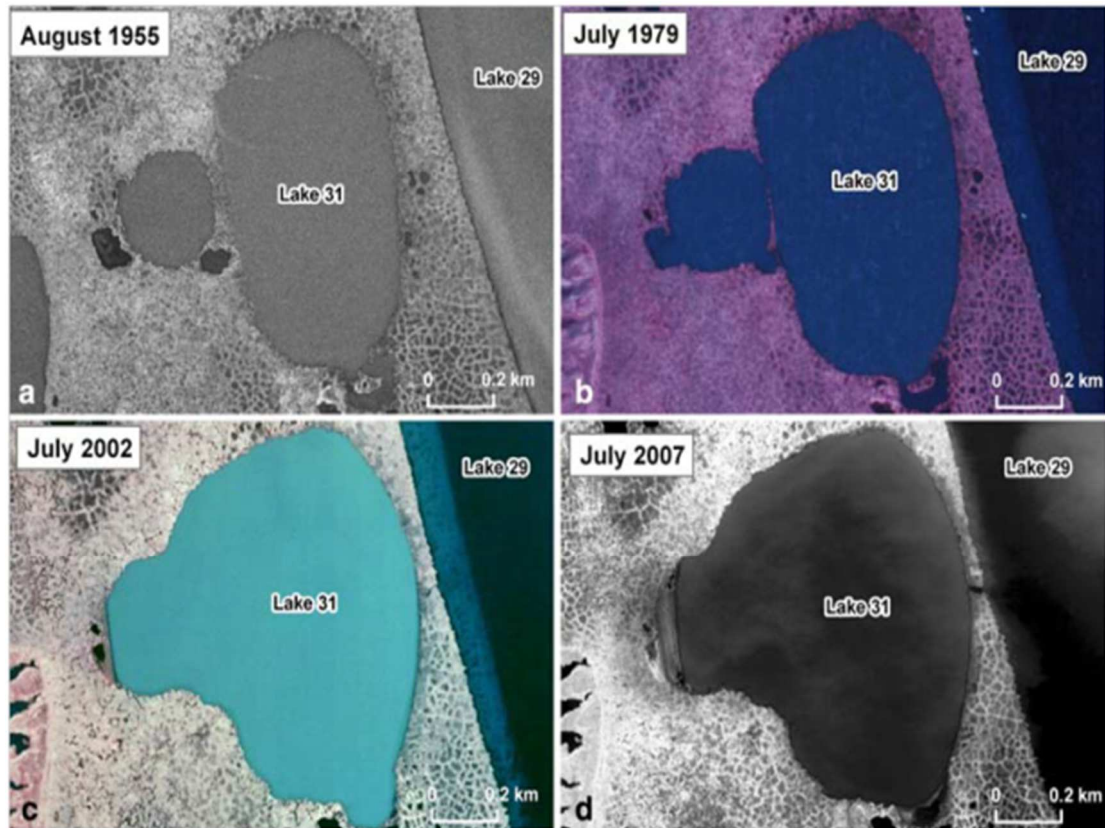


Figure 5. Development of a thaw lake, Alaska. (Jones, Arp, 2009)

3 Study area.

This research focuses on the Alaskan sector of the Arctic; however, general trends in dynamic conditions of permafrost registered in Alaska could be applied for other arctic locations. Alaska is the northernmost state of the United States of America. The state's area is over 660 million square miles, making it the largest state (State of Alaska, n.d.). Figure 6 shows the location of the study area within the state of Alaska.

The size of the study area is 529 km². This study area was selected, because near it the Pumping Station #1 of the Trans-Alaskan Pipeline System is located, and the supporting infrastructure (road network, parking lots, machinery hangars, etc.) is located within the study area. However, the location is not heavily industrialized; it cannot be called an urban area..

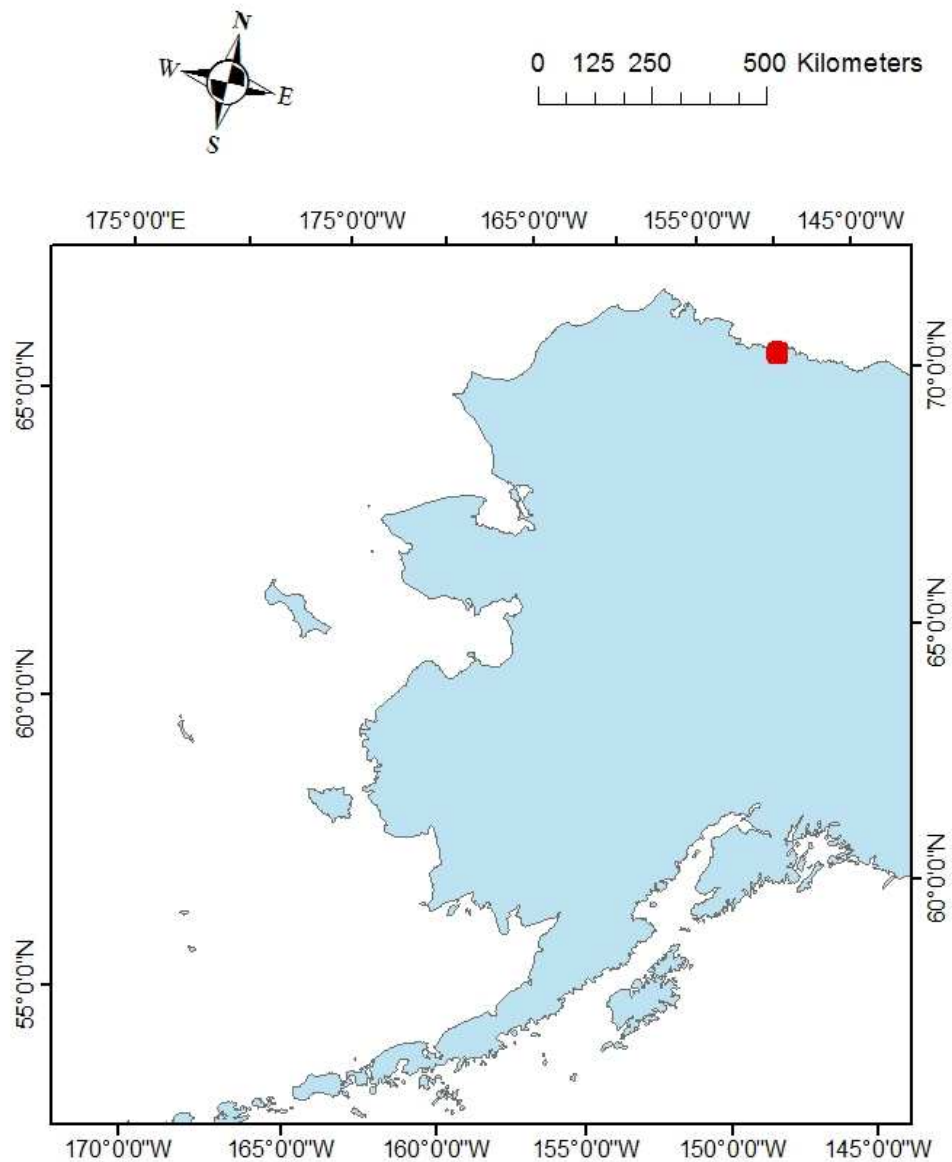
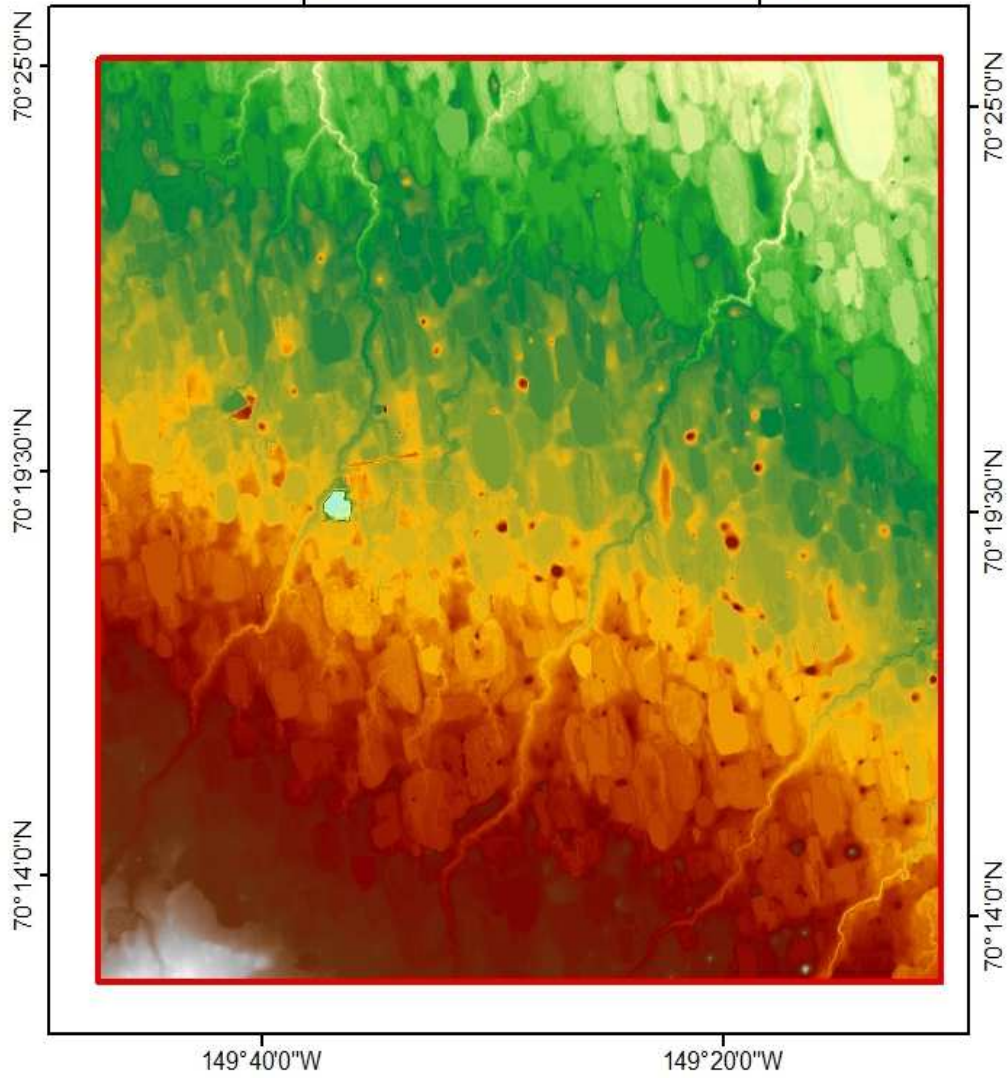
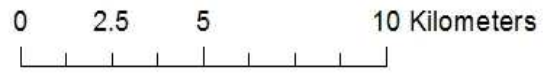


Figure 6. Study area location within Alaska.

The study area is located in the eastern Arctic Coastal Plane of Alaska, at 70° N 149° W, as seen from Fig. 6. Study area occupies The region is underlain continuously by 300–600m of permafrost with high excessive ground ice content (>20% by volume in the upper 10–20 m) (Brown et al., 2002). The area is dominated by tundra vegetation, thaw

lakes, and drained lake basins. The elevation of the area is low, ranging from 0 to 45 m asl (see Figure 7). The elevation data was obtained as the digital elevation model from the United States Geological Survey (2020), and the spatial resolution of this data is 1 m.




Legend

 studyarea

Elevation, m

Value

 High : 44.6803

Low : 0.4

Figure 7. Digital elevation model of the area (DEM courtesy of the U.S. Geological Survey).

There might be local differences in plant communities that affect the development of permafrost beneath them. Arctic tundra vegetation protects and insulates the underlying permafrost; Different plant communities reflect solar insulation differently; for example, mosses are better insulators than shrubs (University of Edinburgh, 2019). However, Arctic vegetation is extremely fragile in itself. Vegetation in the Arctic grows very slow, making it especially vulnerable to long-term disturbance. Damage to the insulating mat of vegetation can cause degradation of the underlying permafrost, followed by thaw and the thaw lake formation (Hinkel et al., 2017).

The urban heat island (UHI) is the phenomenon of ambient temperature being higher in urban areas than in comparable rural areas (Manoli et al., 2019). This happens due to several interrelated factors. Low-albedo, heat-absorbing materials such as concrete, asphalt, and brick are typical for urban environments. The air in urbanized areas is often polluted, contributing to heat retention by lowering air transparency. Although the study area of this research is not heavily urbanized, there may still be the mild UHI effect; Hinkel and Nelson (2007) have registered the temperature increase of up to 2 degrees around the village of Barrow and rural drilling sites. However, in Alaska, the UHI is the strongest in winter and is practically nonexistent in temporarily habitable areas in summer.

The tendency of soils to freeze and thaw, and the rate of that process, is regulated (among other factors) by organic content in it. Polar gelisols tend to contain a lot of organic material (because it does not decompose well in low temperatures). A local difference in organic content in soils can be found, which would justify the difference in permafrost degradation rate. To confirm that, local sampling and analysis of soils must be done, including geochemical markers.

4 Methodology

In this research, the change of permafrost is monitored on the temporal scale to obtain data on permafrost conditions for geotechnical purposes. The rate and direction of change in surface permafrost are determined by measuring and analyzing the presence and parameters of secondary signs of permafrost degradation. By registering the changes in secondary permafrost indicators, such as thaw lakes, the trend of change in underlying permafrost is determined. That gives way to the long-term evaluation of prospects for infrastructure in the region. The key question of this research is to determine whether industrial activities in the Arctic are affecting the condition of surface permafrost. This question is posed because the condition of surface permafrost is the main factor of successful geotechnical engineering in the Arctic. For this reason, the industrial companies are interested in a precise and detailed assessment of permafrost conditions at the ACP.

To meet the goal of the study of determining the direction and rate of permafrost development, secondary signs of permafrost degradation (thaw lakes) were detected, their area measured, and the change of area measured over the 7-year study period. Because satellite images are used in this research without the assessment of borehole data, this research is focusing on the assessment of condition of surface permafrost only, not discussing the deeper layer of permafrost.

Satellite images of the Earth surface within the study area from 8 July 2013 and 01 August 2020 were obtained from the EarthExplorer portal (United States Geological Survey, 2019). The Landsat-8 satellite imagery was chosen because its spectral resolution allows for calculating the modified Normalized Differentiation Water Index (NDWI); the Operational Land Imager sensor (OLI) of Landsat-8 delivers images in two spectral bands required for the calculation of NDWI (Mondejar, 2019). The spatial resolution of images from the OLI sensor is 30 m by 30 m. The time when both sets of images were taken corresponds to the middle of the thaw season. It was important to analyze images during the thaw season after the spring ice removal events. By the middle of the thaw season, the water balance in lakes becomes relatively stable (Hinkel et al., 2017)

Additional data was used in this research to assess the spatial distribution of the thermokarst lakes within the study area. The map of permafrost types with excessive ground ice content was obtained from Brown et al (2002). The map of road network in the area was obtained from the State of Alaska Open Geodata Portal (2020).

To calculate the NDWI values over the study area for different years, spectral composites of bands 3 and 5 were made for the study area. The composite raster image was created using ERDAS Imagine ver. 16.0, utilizing the Layer Stack tool. Then, the NDWI was calculated according to McFeeters (1996) over the whole study area.

4.1 Normalized Difference Water Index

The main research method is the Normalised Difference Water Index (hereinafter NDWI), used to detect open water features in satellite images. Initially, the method was proposed for the detection of moisture in vegetation (Gao, 1996). The index is calculated by the formula below:

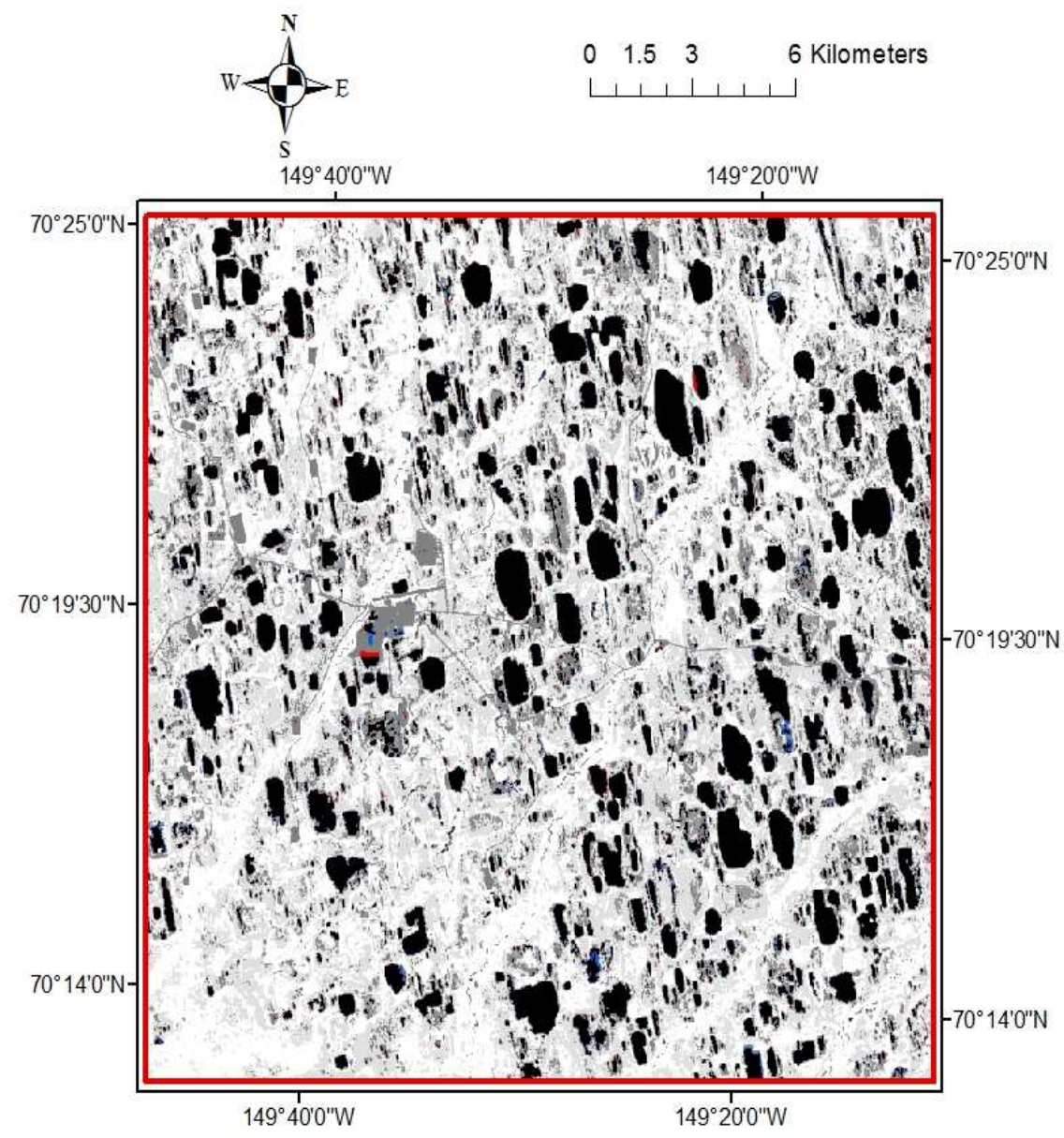
$$NDWI = \frac{X_{NIR} - X_{SWIR}}{X_{NIR} + X_{SWIR}}$$

where X_{NIR} is the pixel value of the near-infrared wavelength band, and X_{SWIR} is the pixel value of the short wavelength infra-red band. The variation of this method described by McFeeters (1996) is adjusted for detecting open water in large bodies. The formula of the index uses the green and infrared wavelength bands. The adjusted formula is presented below:

$$NDWI = \frac{X_{green} - X_{NIR}}{X_{green} + X_{NIR}}$$

where X_{green} is the pixel value of the green wavelength band, and X_{NIR} is the pixel value of the near-infrared band. For data from Landsat-8, X_{green} corresponds to spectral band 3, and X_{NIR} corresponds to spectral band 5. Spectral band 3 of the OLI sensor of Landsat-8 is 0.53-0.59 μm , which corresponds to the green color of visible spectrum; spectral band 5 is 0.85 - 0.88 μm , which corresponds to the near-infrared part of the electromagnetic spectrum.

The method of lake detection by NDWI was chosen because it allowed for clear identification of thaw lakes with open water and drained lake basins, which are often represented by patches of wetland. Negative values of NDWI mean dry land, and positive values mean open water, according to McFeeters (1996). As seen in Fig. 8, where open water is shown in black, areas of wetland are often seen around lakes (shown in dark grey); these are the drained lake basins that retain excessive soil moisture and become wetlands. By using the proposed method of open water detecting via NDWI, the significant patterns in the tundra landscapes can be seen - the abundance of thaw lakes and associated drained lake basins.



Legend

 studyarea

NDWI values:








	-0.337730676 - -0.23429191		-0.116914868 - 0
	-0.23429191 - -0.195502372		
	-0.195502372 - -0.136394506		
	-0.136394506 - 0		
	0 - 0.133285135		0 - 0.197696731

Figure 8. Combined map of NDWI values of 2020 (dry land) and 2013 (open water).

Figure 8 is the combined image of NDWI from 2020 and 2013. The image was obtained using ArcGIS ArcMap Desktop ver. 10.8.1. The Extract by Attributes instrument was used to extract the pixels with values above 0 from the 2020 scene, which are the thaw lakes containing open water. Then, using the lake area mask from 2020, part of the 2013 scene was extracted. In the extracted image, most pixels had positive values (representing open water), because they correspond with open water pixels from 2020; however, some pixels in the extracted image have negative values – these are the pixels that were filled with water in 2013 but dried up by 2020. Such pixels are depicted in Fig. 12 with red color, and that is the negative change of lake area from between 2013 and 2020.

The extracted 2013 image with lake areas and red pixels was mapped against the full 2020 NDWI scene, and pixels with values above 0 are filled with blue color. Most of the lake area in the 2020 scene was covered by the 2013 lakes. However, some blue pixels are still visible – those are the areas that were dry land in 2013 but got covered with water by 2020.

4.2 Lake Depiction

In order to assess the spatial distribution of lakes with different parameters, the following procedure was performed. The areas with pixel values above 0 were extracted from the 2020 scene, creating a single-polygon layer. Then, that layer was transformed into line features and back into polygons to create a layer with multiple polygons corresponding to thaw lakes in the scene. Centroids were created for the polygons and added to the layer's attributes table using the Join Table tool. The same procedure was performed for the 2013 scene.

Then, the Spatial Join tool was used to join the layers and link the polygons of the same lake between the years. The 2013 layer was joined with the 2020 layer. The option of `HAVE_THEIR_CENTER_IN` was used, because it matches the features in the join features with the target features, if a target feature's center falls within them, according to Arcgis.com (2020). That allowed for the comparison of lake area and calculation of the growth rate in percent.

5 Results

The total number of identified lakes varies by year; all detected areas were taken into consideration as lakes. In 2013, there were 2833 polygons identified as lakes (bearing open water); In 2020, there were 2787 lakes identified, which signifies the 1.62% decrease in the number of lakes over the years. Simultaneously, the total area of open water for the study area has increased from 76105800 m² in 2013 to 77387400 m² in 2020, showing an increase of 1.67%.

Thaw lakes are divided into 14 classes according to their size (see Table 1). Figure 9 shows the histogram of lake sizes by count. As seen from the figure, most detected lakes (around 1300 lakes in both 2013 and 2020) are the smallest in size (below 2000 m² in area, which is only 2 cells according to the spatial resolution of the OLI sensor of Landsat-8). These small lakes can be considered the ponds from which the full thaw lakes may form. Smaller lakes are more abundant than the large ones; the bigger the size, the less lakes of that size are within the study area.

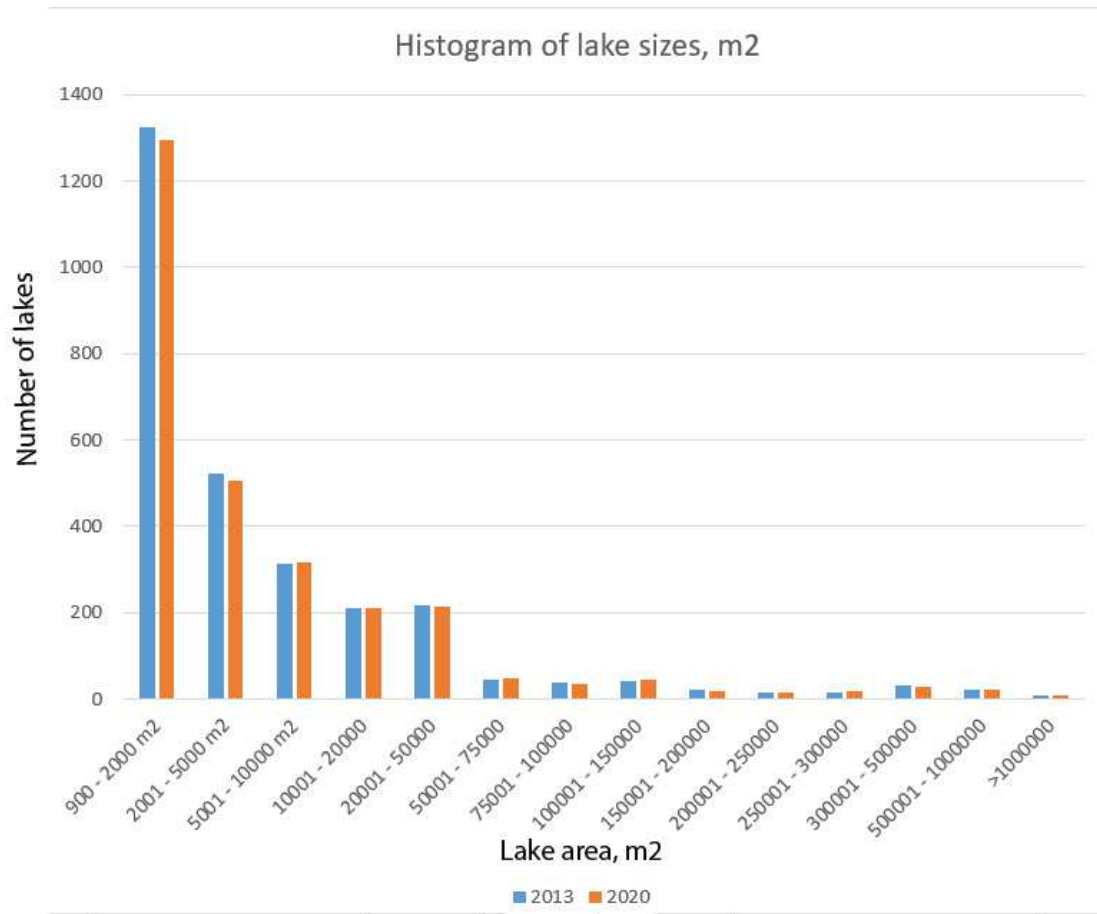


Figure 9. Histogram showing the distribution of lake area.

Table 1. Lake area statistics

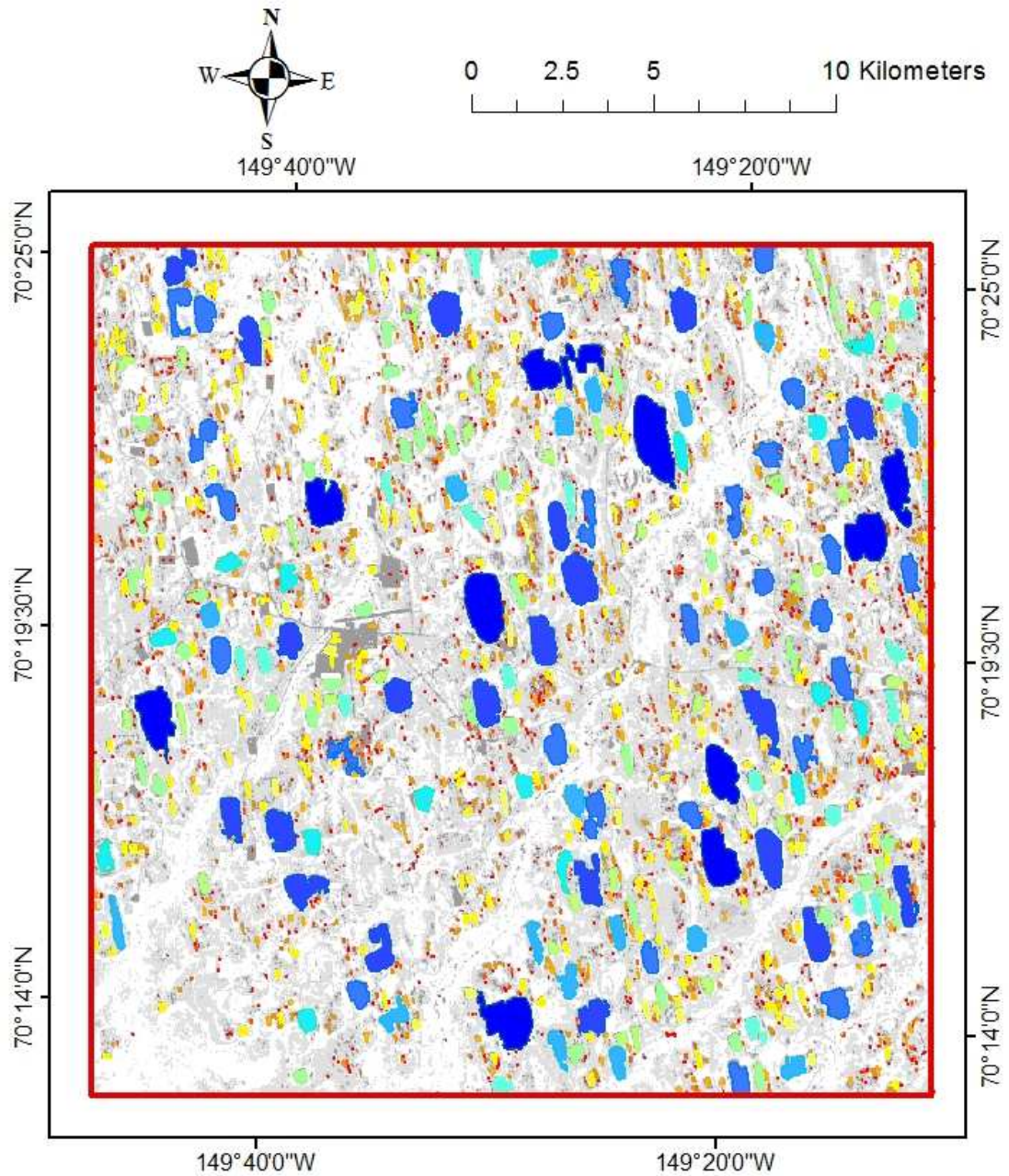
	2013	2020	d	d%
total area of water, m²	76105800	77387400	1281600	1.68
total number of lakes	2833	2787	-46	-1.62
total number of lakes by area (m²): 900 - 2000	1324	1295	-29	-2.19
2001 - 5000	523	507	-16	-3.06
5001 - 10000	315	316	1	0.32
10001 - 20000	212	211	-1	-0.47

20001 - 50000	217	214	-3	-1.38
50001 - 75000	46	49	3	6.52
75001 - 100000	40	36	-4	-10.00
100001 - 150000	41	44	3	7.32
150001 - 200000	21	20	-1	-4.76
200001 - 250000	16	16	0	0.00
250001 - 300000	17	18	1	5.88
300001 - 500000	31	30	-1	-3.23
500001 - 1000000	21	21	0	0.00
>1000000	9	10	1	11.11

The lakes occupy 14.1% of the total study area in the 2013 scene, compared with 14.4% in 2020. The distribution of the lakes by area is shown in Fig. 13. As seen from the figure, most of the lakes have areas from 900 to 10 000 000 m². However, the cumulative area of these lakes decreases from 2013 to 2020, and the area of bigger lakes increases, as shown in Table 1. Together with the fact that the cumulative area of open water in the study area has increased, it may mean that small lakes grew in the area over time and upgrade the size class.

Small lakes may also merge to form larger lakes. The smallest lakes that can be detected in this analysis have 900 m², which is limited by the spatial resolution of the Landsat-8 data (United States Geological Survey, 2019); however, there may exist smaller ponds in the tundra. From Fig. 10 it is seen that lakes of any size are scattered within the area; none of the size classes of lakes demonstrates patterns of regulated distribution.

There are no large lakes above 300000 m² in the south-eastern corner of the study area, where underlying permafrost is of type with low ground ice content (Brown et al, 2002).



Legend

 studyarea

2020 lake area, m²

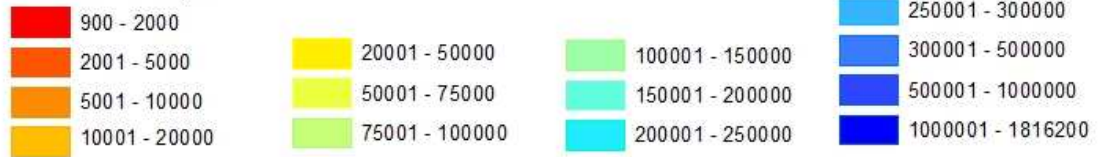
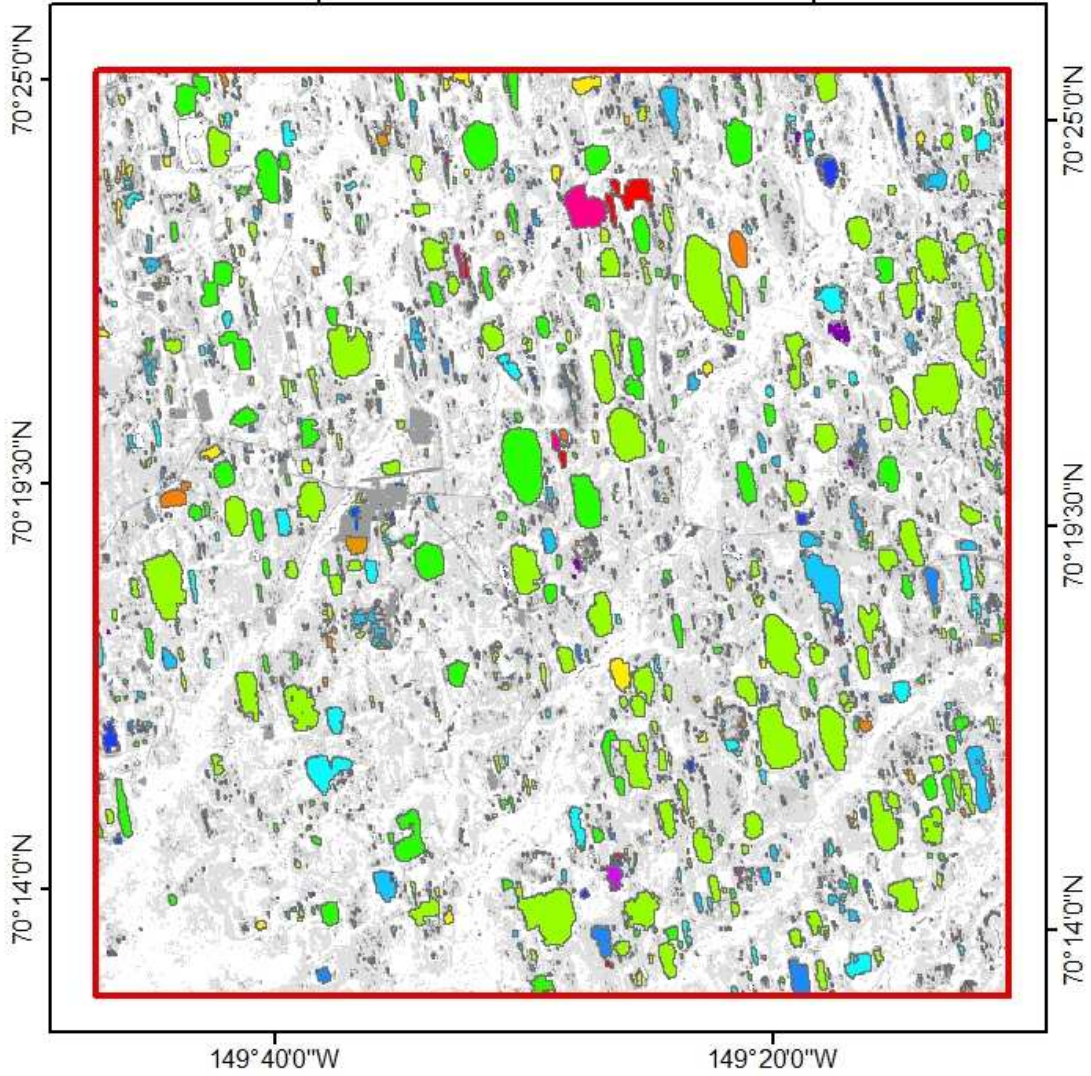


Figure 10. Spatial distribution of lake size according to Table 1 (year 2020).

5.1 Lake Growth Rate

The Spatial Join tool of ArcGIS Desktop ver. 10.8.1 was used to compare the area values between the scenes from different years; the join was performed using the option of joining the centers of polygons (see the Methodology section). The rate of change in area was calculated for each lake in percent. According to the rate calculation procedure, only 912 lakes (32% of all lakes) were registered to have an area change within the study period. Figure 11 demonstrates the distribution of lakes by the rate of change. The histogram of lake count by rate is shown in Figure 12. Lakes with rate of change over 100% were separated into a common class. Lakes with negative growth rate below -75% are rare, most of the shrinking lakes have the shrinkage rate between -50% and -5% (264 lakes); there are 130 lakes with growth rate from -5% to 5%; and the majority of the lakes have growth rate above 5% (518 lakes). That signifies the general increase on open water area with the study area. Two large lakes in the north of the study area, shown in red and magenta in Fig. 11 have huge growth rate of 100% and above,



Legend

studyarea

Change rate, %

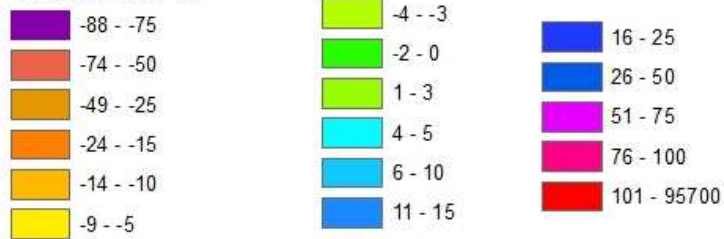


Figure 11. Spatial distribution of the thaw lakes by growth rate by 2020.

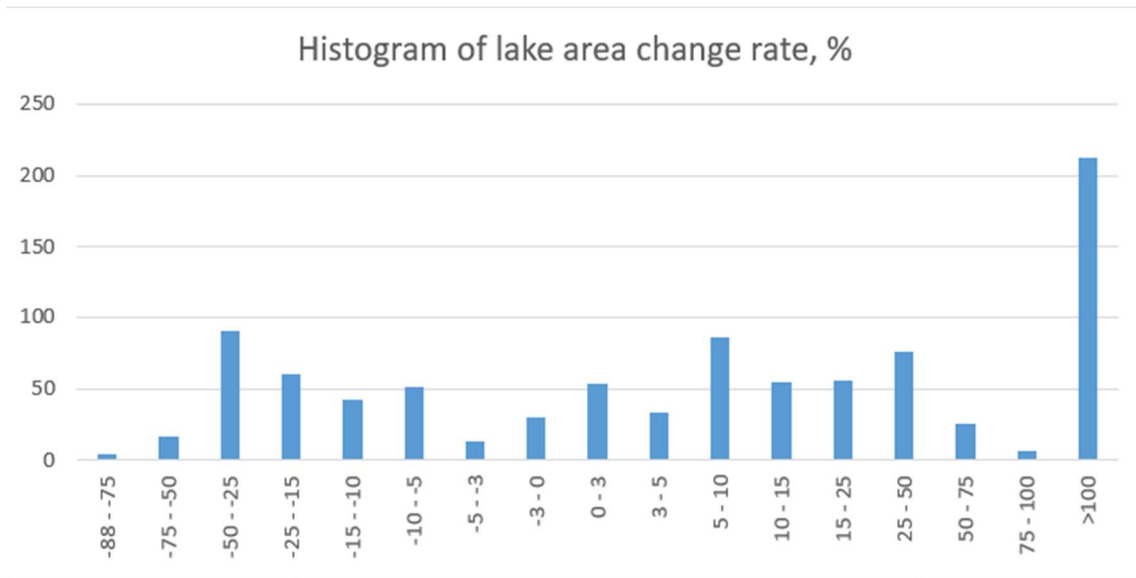


Figure 12. Histogram of lake area change rate in percent.

As seen from Figure 12, large lakes mostly have a low growth rate between -5% and 3% over the study period, whereas small lakes have substantial positive growth rates. That is because small lakes tend to merge into larger lakes. However, because the lake areas are compared polygon by polygon by the ArcGIS software (Arcgis.com, 2020), as described in the Methodology section, the growth rate shows the merged lakes as small lakes having the growth rate over 500%. Figures 13-15 show the verification of the growth rate in individual lakes: area values are given in Table 2. The lakes were randomly selected from the lake list. As seen from Table 2, lake 1 had the area of 1800 m² (2 pixels) in 2013, but in grew by 50% and reached the area of 2700 m² (3 pixels). Lake 2 had the area of 1800 m² (2 pixels) in 2013, but the area got 50% less and reached the area of 900 m² (1 pixel). Lake 3 had the area of 1800 m² (2 pixels) in 2013, and the area grew by 50% and reached 3600 m² (4 pixels). Verification was performed to assure the accuracy of the lake depiction method.



0 0.01 0.02 0.04 Kilometers

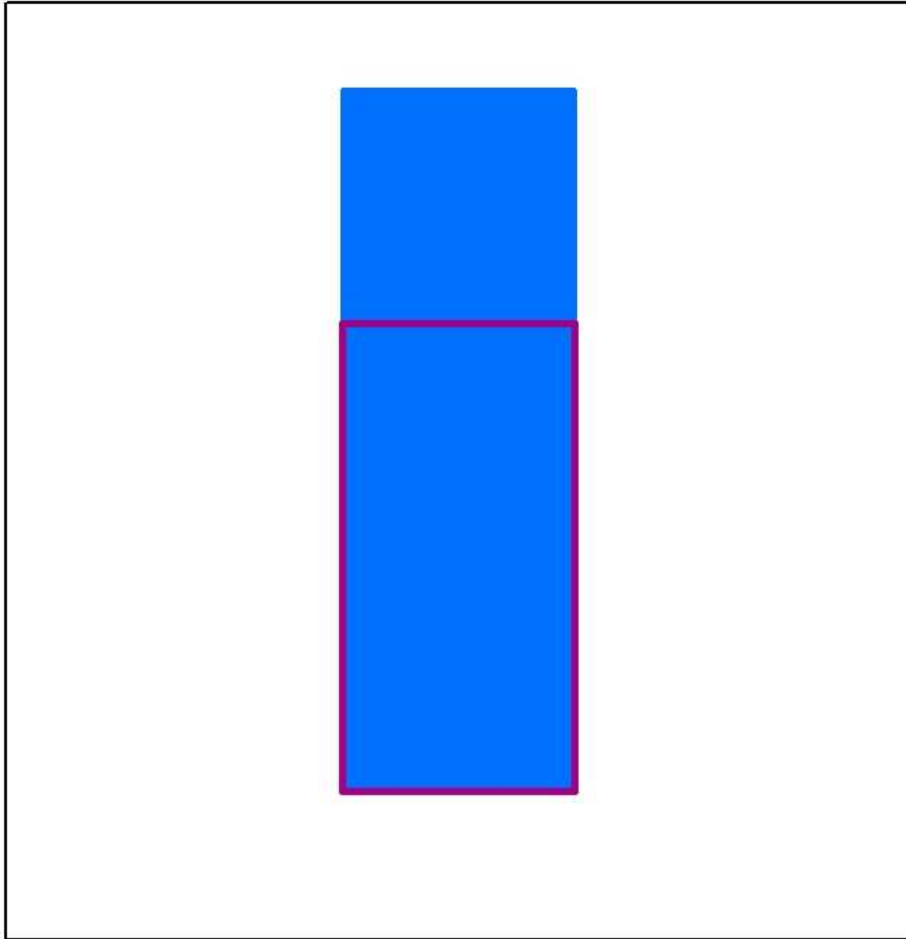


Figure 13. Verifying the area assessment for lake 1 (2013 area is the outline, 2020 area is filled)

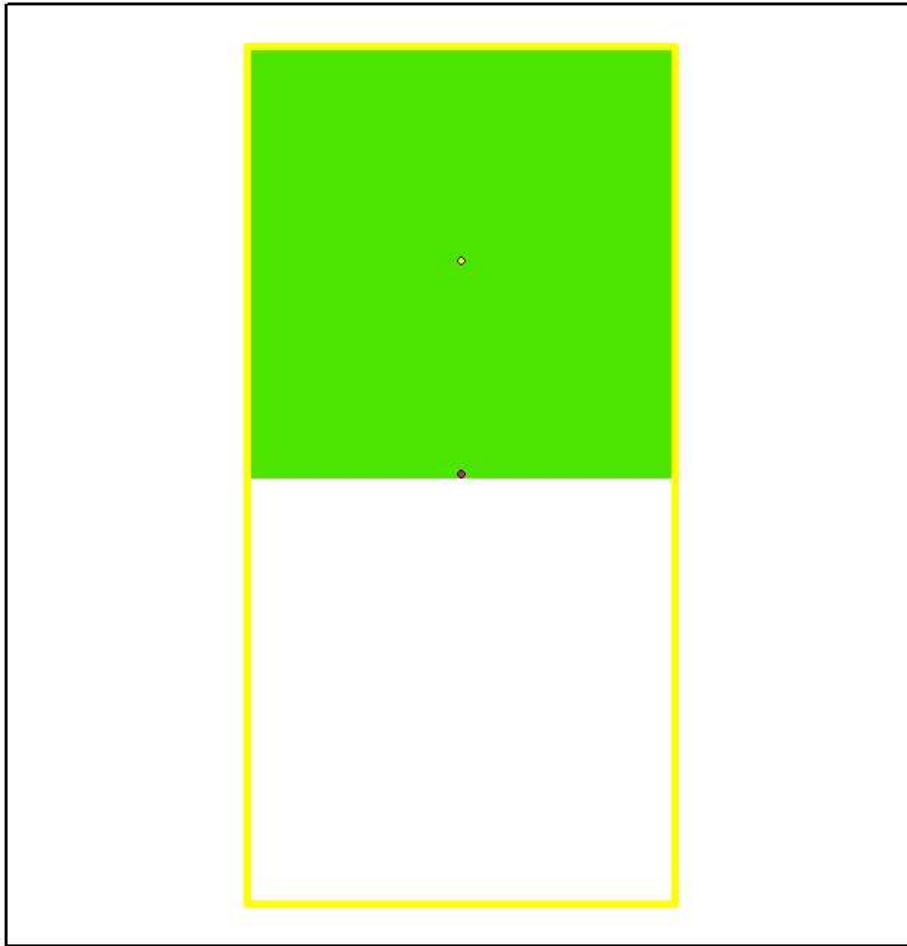
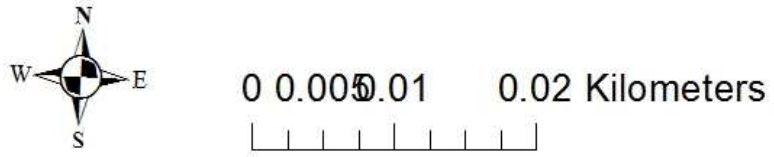


Figure 14. Verifying the area assessment for lake 2 (2013 area is the outline, 2020 area is filled).

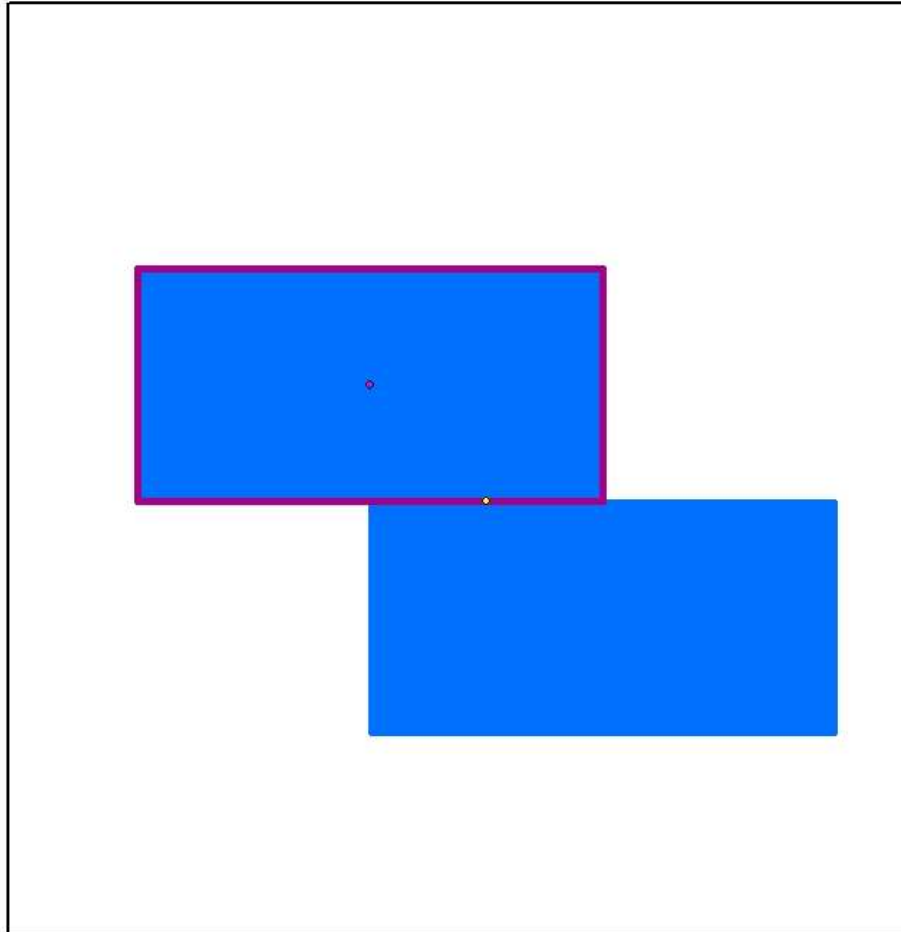
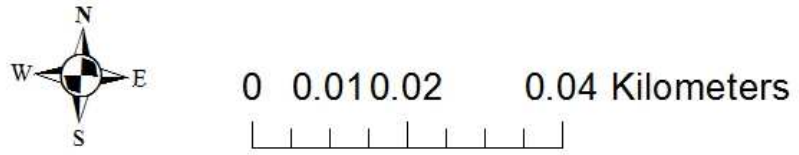


Figure 15. Verifying the area assessment for lake 3 (2013 area is the outline, 2020 area is filled)

Table 2. Checking the assessment of sample lakes.

N	2013 area, m2	2020 area, m2	Growth rate, %
1	1800	2700	+50
2	1800	900	-50
3	1800	3600	+100

Because of the process of thaw lake formation, small lakes and ponds are shallow and are more likely to change their area due to annual fluctuations in precipitation, therefore even a huge change in their area is likely to be the result of temporary factors. For larger lakes that are deeper, annual fluctuations in precipitation have less impact. Significant change in area in large lakes over 5000 m² (over 4500 m², which is 5 pixels according to the implemented spatial resolution) is more likely to be caused by either the geomorphological changes due to permafrost degradation or anthropogenic influence.

Because the change of area in percent is a relative number, the change in area was also calculated in pixels (cells) for each lake, one pixel is 900 m². The change in area was determined significant if it was more than 5 pixels during the study area. Figure 16 shows the scatter plot of lake area change in pixels versus the lake area by 2020. Only lakes that are larger than 5000 m² and that have the rate change over 5 pixels are included in the selection, and there are 1092 lakes that fit the selection within the study area. As seen from the figure, most lakes have the 2020 area below 600000 m² and the growth in area of less than 200 pixels. The first visible trend in the graph is that both small and large lakes have low area change pixel counts (the linear gathering of dots along the horizontal axis).

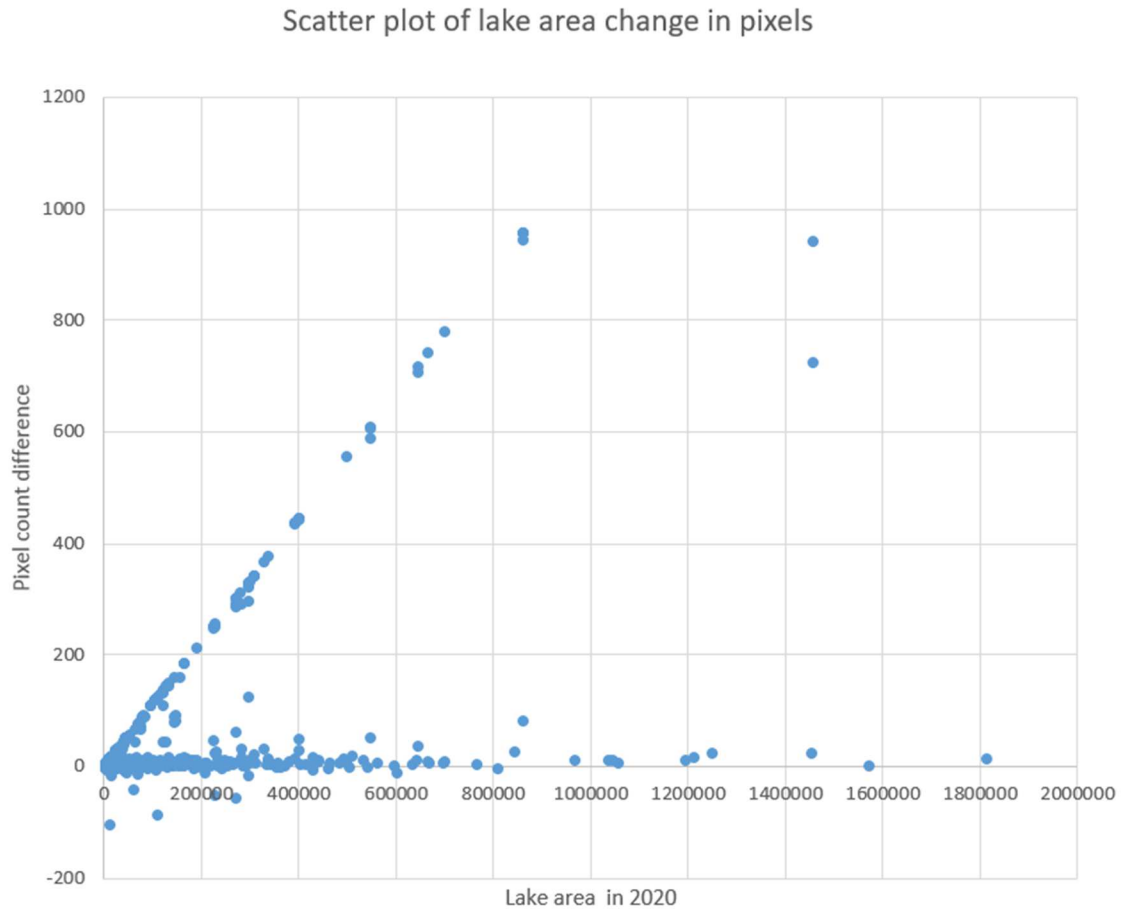
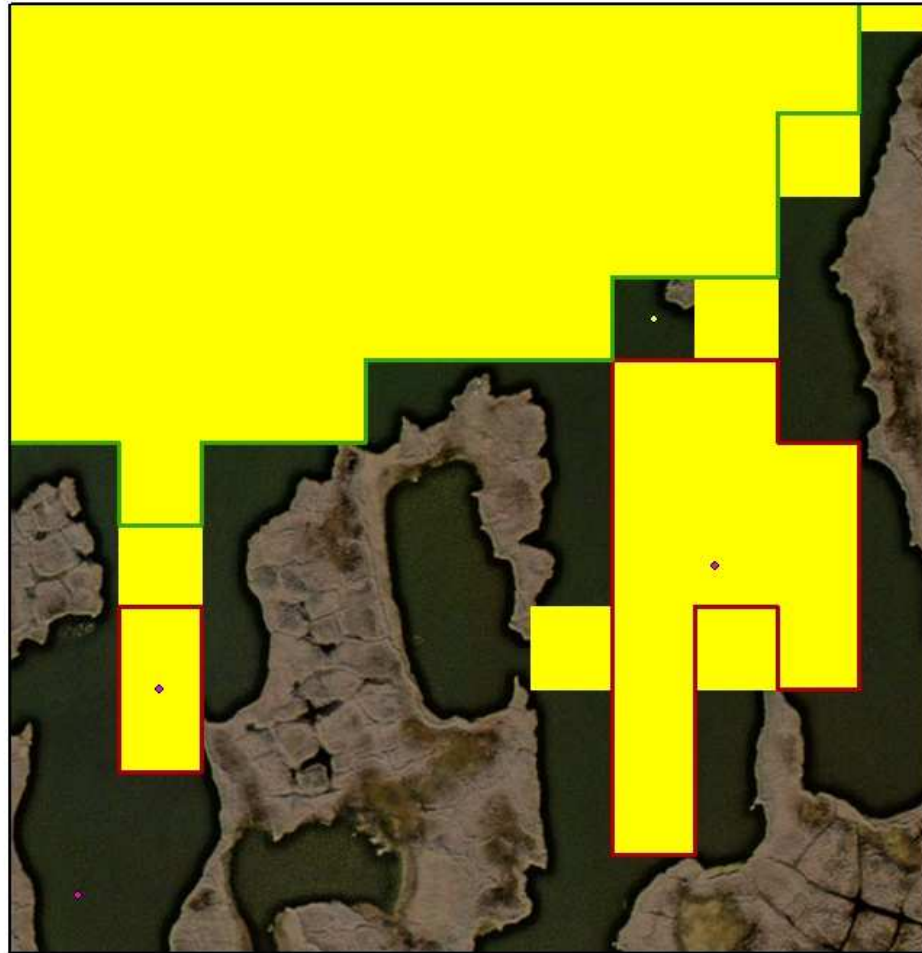


Figure 16. Scatter plot of lake area change in pixels.


In Fig. 16, there's also a trend visible, where in some lakes, growth amount in pixels increases proportionate to the increase in lake area. According to the graph, for the points in this group, the added area (change in pixels multiplied by 900 m², which is the size of 1 pixel) is almost equal to the 2020 area of the lake. Therefore, before the huge increase in area, these lakes must have been very small. For example, in Figure 17 it is seen that in 2013, there were two small, isolated water bodies (outlined in red) in the middle of the scene. By 2020, they got filled more with water and merged with the bigger lake (outlined green, to the north), forming a single water body. Therefore, according to the method of calculation, smaller lakes were reported to have an increase of area the size of the big lake that has incorporated them. This explains the diagonal trend in Fig. 16.




0 0.0325 0.065 0.13 Kilometers





Legend


 big lakes 2020

Difference in cell count

 -105 - -42

 -41 - -20

 -19 - -5

 -4 - 5

 6 - 17

 18 - 34

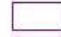
 35 - 61

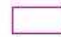
 62 - 91

 92 - 147

 148 - 211

 212 - 300

 301 - 376

 377 - 607

 608 - 957


Figure 17. Merging of small lakes with a large one.




0 0.15 0.3 0.6 Kilometers





Legend


 big lakes 2020

Difference in cell count

 -105 - -42


 -41 - -20

 -19 - -5

 -4 - 5

 6 - 17

 18 - 34

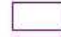
 35 - 61

 62 - 91

 92 - 147

 148 - 211

 212 - 300

 301 - 376

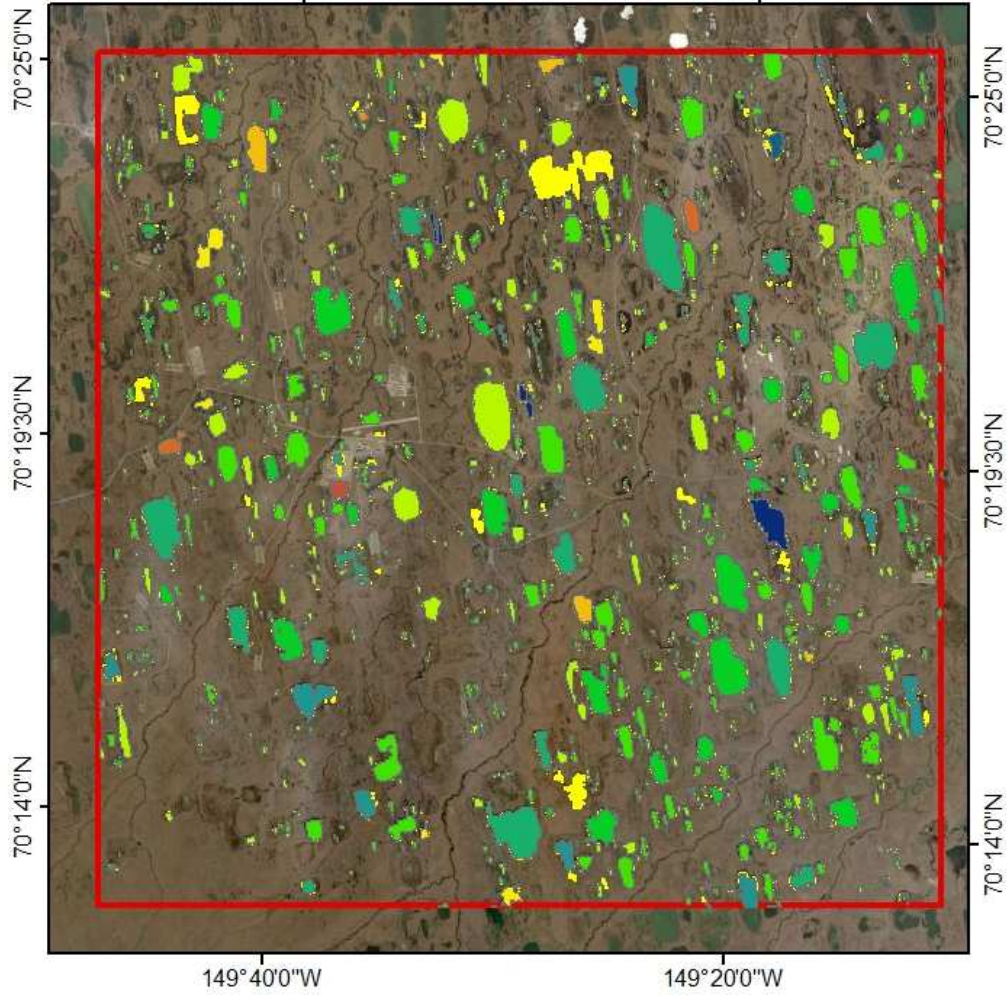
 377 - 607

 608 - 957

Figure 18. Merging of small lakes with a larger one.

Due to this limitation to the calculation method, the lakes in the main area of Fig. 16 were assessed as the true large lakes within the study area. According to Fig. 9 the lakes were chosen, that have the 2020 area above 5000 m², and the pixel change below 100 pixels, to eliminate the points in the diagonal trend and cover the truly changing large lakes.

Figure 19 shows the map of lakes with areas over 5000 m² (0.5 ha) in 2020, and the change in pixel count below 100 pixels. As seen from the map, most lakes have pixel change counts between -4 and 35 (their outlines are orange, yellow and green). Some lakes are shown to have the higher pixel change (shown in magenta and red); those are also attributed to the merging of multiple lakes; the large lake shown in blue in the eastern half of the image is the lake from Fig. 16. Figure 19 shows the histogram of area change in pixels, according to the classification in Fig. 20. As seen from both figures, most lakes have undergone very small change in area from -5 to 5 pixels. More lakes have positive growth rate.



Legend  studyarea

Cell difference

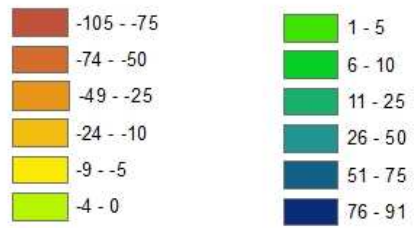


Figure 19. Lakes over 5000 m² and their change in pixels below 100.

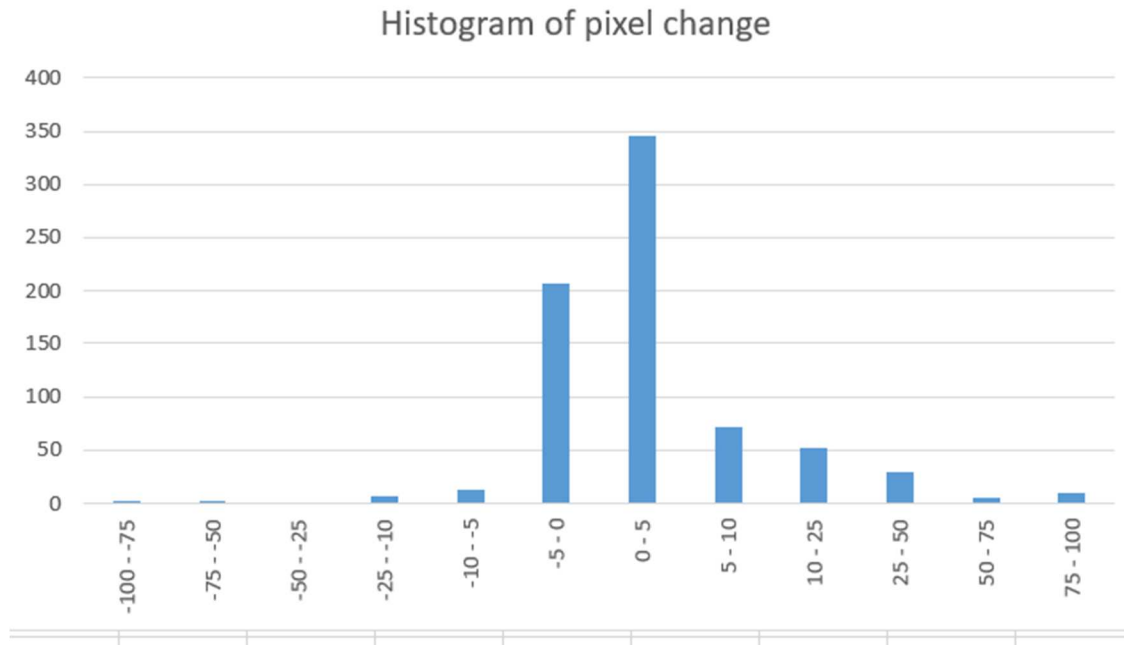


Figure 20. Histogram of area change in pixels.

Figure 21 shows the scatter plot of the change rate in pixels in lakes over 0.5 ha versus the lake area. Total number of identified large lakes is 1029. As seen from the figure, most lakes follow the main trend, where lakes of all sizes have relatively low area change: 1006 lakes have the area change between -50 and 50 pixels (45000 m²), 964 lakes have the area change between -20 and 20 pixels (18000 m²), and 700 lakes have the area change between -5 and 5 pixels (4500 m²). 566 lakes grow in size, 266 lakes do not have the registered change in area, and 246 lakes shrink in size. Therefore, the average growth rate for large lakes can be calculated for the study area: it equals 3.62 cells (3258 m²) per lake over the study period, or 435 m² per year. It equals an area 20 m by 20 m, which can be significant for a lake of 5000 m².

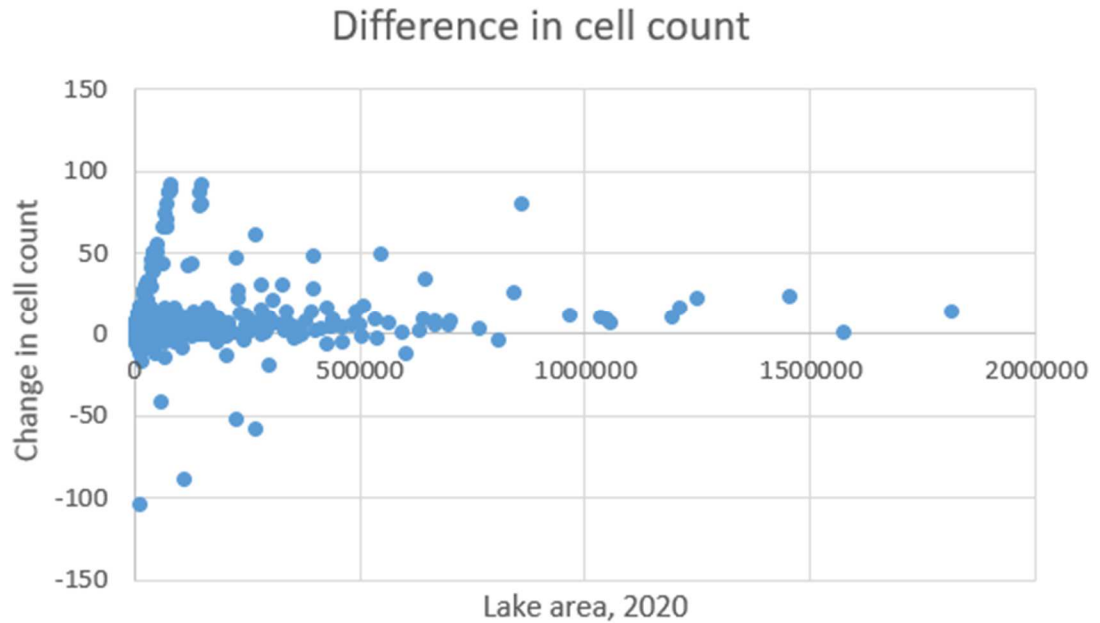
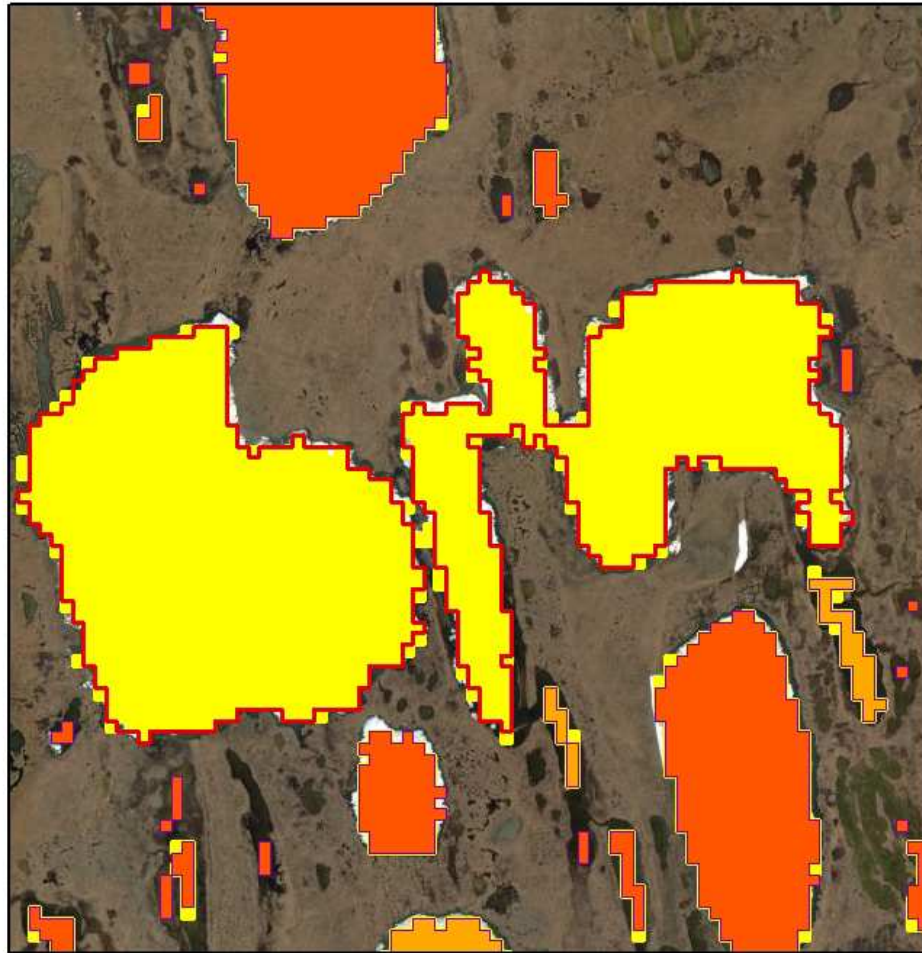


Figure 21. Difference in cell count versus the lake area (m²).

During the research, it has been noticed that some larger lakes show the extreme change in area. For example, in Figure 22 there is one large lake shown in yellow in the middle of the scene; the red outline shows that in 2013 there were two separate lakes. Therefore, the lakes have merged by 2020; due to the methodology aspects, each lake in 2013 was considered to have an increase in area equal to the second merging lake. Both lakes were shown to have a huge increase in area, when in reality, they have merged together. There has formed a channel in the thawed ground between the lakes; this means that there has been degradation of permafrost on the site. The increase in the area of lakes was determined by the research method as huge, however, in reality the lakes haven't expanded much.



0 0.25 0.5 1 Kilometers



Legend

Difference in cell count

608 - 957

lakes over 0.5 ha

Figure 22. Merging of two lakes over 0.5 ha.

5.2 Examples of lakes

To demonstrate the results of the applied method, series of images were created, depicting a few lakes before and after the study period. In the Figure 26, a lake is depicted. In this and the following figures, image A shows the visible spectrum image of the lake, composed from the Landsat-8 satellite images from 8 July 2013 (USGS.gov, 2020). In image B, there is the image of the same lake on 01 August 2020. The resolution of the Landsat-8 images is 30 m by 30 m. Image C depicts the high-resolution visible spectrum satellite image of the same lake, obtained from the Alaska Mapping Executive Committee (2020). Unfortunately, this data is only available for 2020, so it was impossible to use high-resolution images in the main method. The spatial resolution of this image is 0.5 m by 0.5 m.

From the Fig. 23 it is seen that the detection of the lake's exact size is difficult in the visible spectrum. The results of the applied method are based on the NDW calculations. During the NDWI lake detection, the algorithm may attribute pixels to open water, which do not appear like that in the visible spectrum images. Therefore, the verification of the NDWI detection method is difficult using the visible spectrum images in the same resolution. For better verification, high-resolution images should be assessed from both 2013 and 2020. Another way to improve the method is to perform the calculation on high-resolution images initially; that is, if such are available for both the beginning and the end of the study period.

In Fig. 23, the lake was detected to have grown by 8%, adding 10 cells. Its area has changed from 107089 to 116100 m². In images A-B, the intensity of color is higher in 2020, and new pixels are shown in dark color; since open water normally looks dark in visible spectrum, it can be inferred that the area of open water has increased.



0 0.15 0.3 0.6 Kilometers

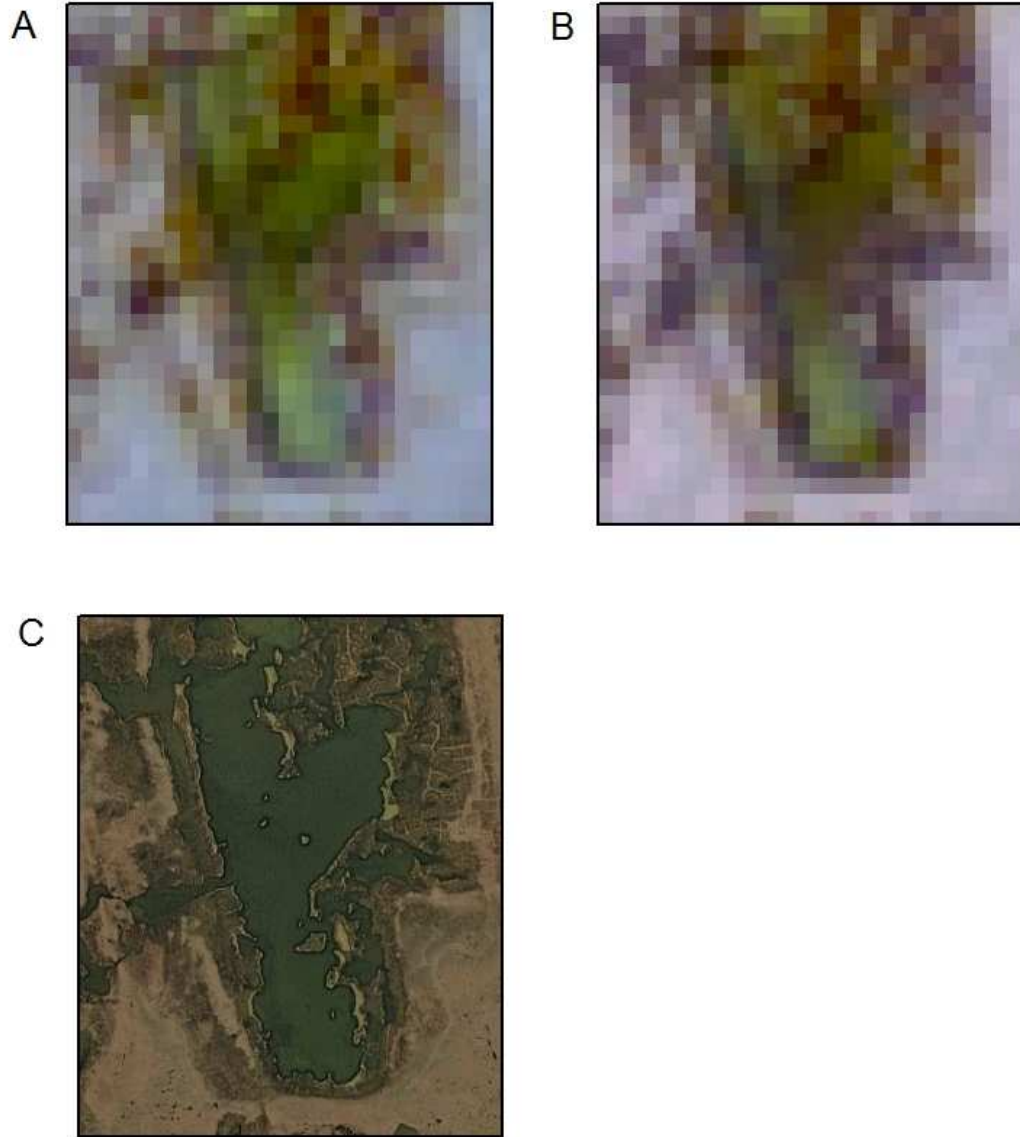


Figure 23. Example of a moderately grown lake; A – 2013, B – 2020, C – high resolution 2020.

In Figure 24, the lake was detected to have grown by 9%, adding 5 cells. Its area has changed from 51300 to 55800 m². Just as in the previous example, in images A-B, the intensity of color is higher in 2020, and new pixels are shown in dark color; since open water normally looks dark in visible spectrum, it can be inferred that the area of open water has increased. This lake is located near a building; its drainage passages may have been disrupted during construction. In the figure, the snow fence is visible (the angled white structure in the south east of the lake; the snow fence was most likely installed to protect the nearby infrastructure from getting buried under snow in winter. The installation of the fence may have interrupted the drainage system of the lake, blocking its drainage channel, what might have caused the accumulation of excessive water in the lake, increasing its area.

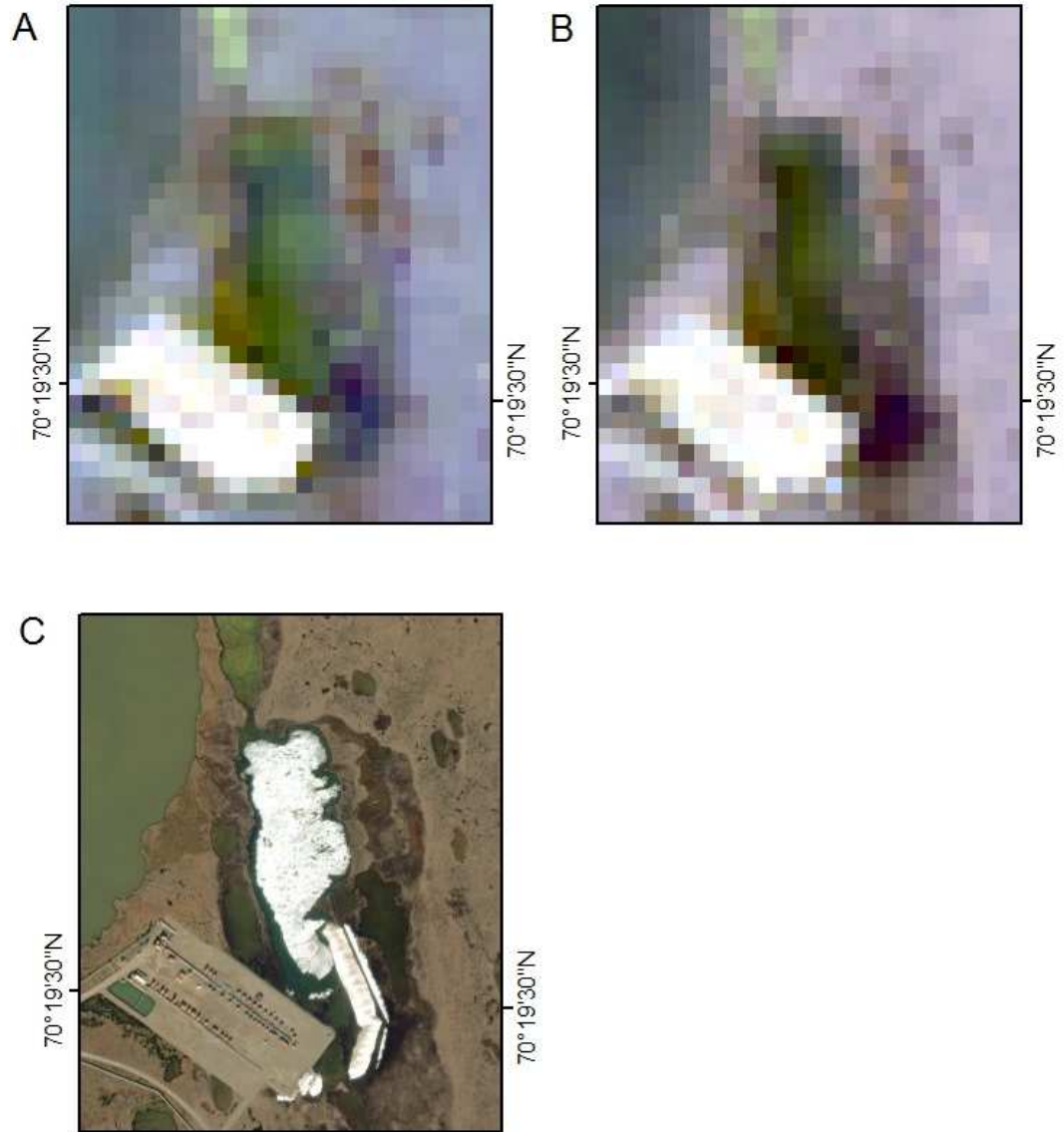


Figure 24. Example of a moderately grown lake; A – 2013, B – 2020, C – high resolution 2020.

In the Figure 25, the lake was detected to have grown by 9%, adding 8 cells. Its area has changed from 81000 to 88200 m². As in the previous figures, images A-B, the intensity of color is higher in 2020, and new pixels are shown in dark color; since open water normally looks dark in visible spectrum, it can be inferred that the area of open water has increased.

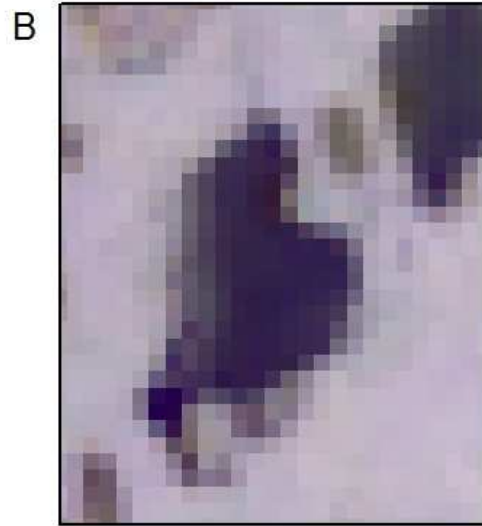
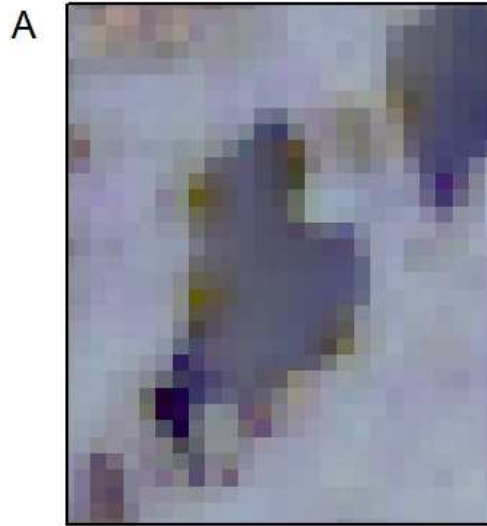


Figure 25. Example of a moderately grown lake; A – 2013, B – 2020, C – high resolution 2020.

The following examples feature individual lakes from the study area that have been observed to have huge area change, according to Fig. 20. In the Figure 26, the lake was reduced by 17%, losing 53 cells. Its area has changed from 277290 m² to 229199 m². As seen from the figure, there are two lakes joined by a channel. However, the NDWI method has not detected the channel in the 2020 image. Therefore, the bigger lake was detected to have lost its north-eastern part, hence the detected reduction.

However, in the high resolution 2020 image the channel is clearly seen. This example shows that this method of detecting open water has limitations. When it returns area change values significantly higher in amplitude than the average for the area, it may signify that the detachment has happened; at the same time, as seen in this example, the detachment may have not happened. It is recommended to manually check the lakes in which there were outlying changes detected. This assumption is supported by the next example.



0 0.175 0.35 0.7 Kilometers

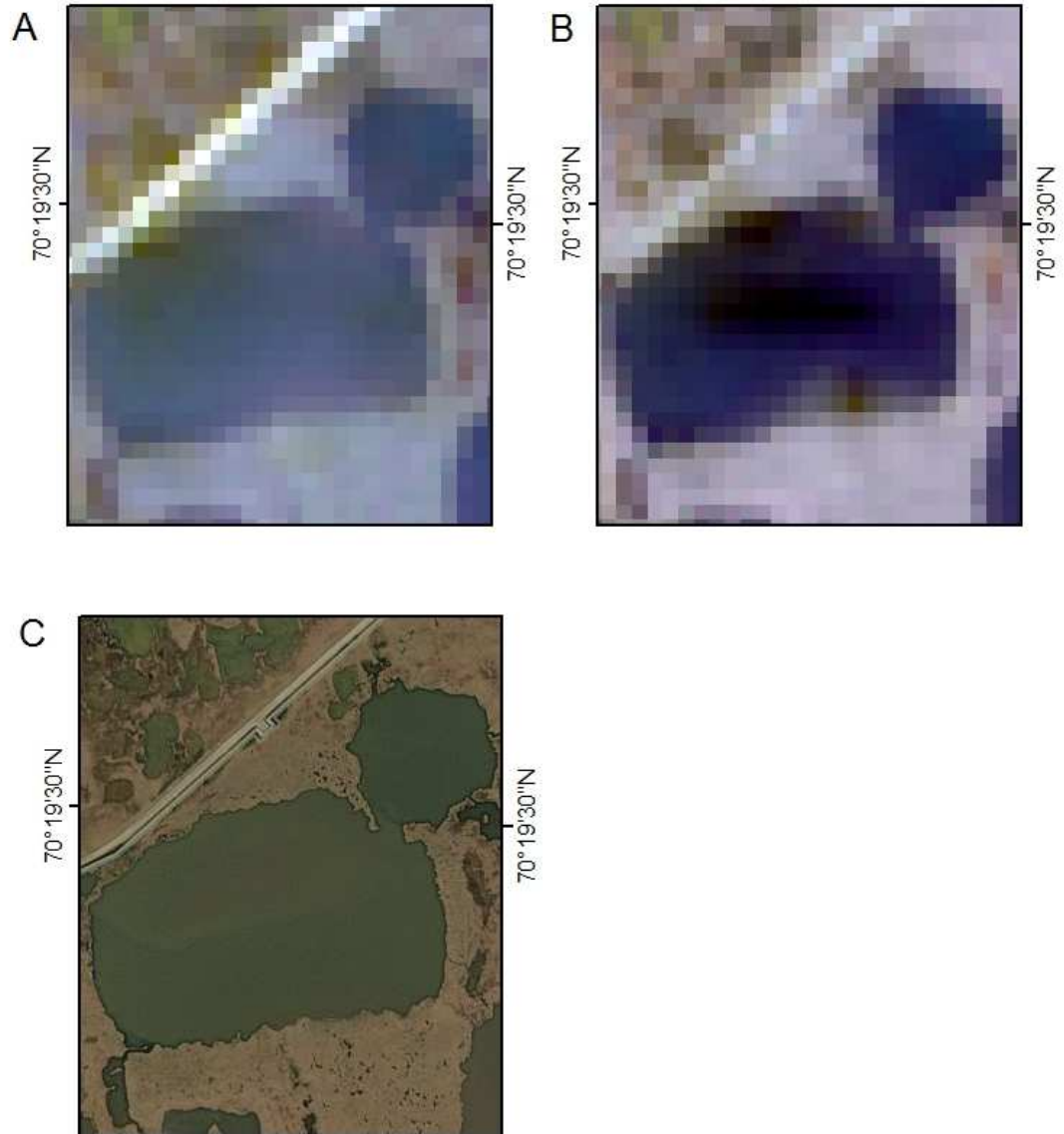


Figure 26. Example of a significantly shrunk lake; A – 2013, B – 2020, C – high resolution 2020.

In Figure 27, the lake has grown by 121%, adding 91 cells. Its area has increased from 62500 to 149400 m². As seen in the scenes A and B, the lakes might be seen as connected. However, it is seen that the channel connecting the two lakes looks less prominent in the 2013 image (scene A). It appears that the NDWI detection method has not detected the channel in 2013 but has detected it in 2020. Therefore, the lake was attributed as newly merged with a neighboring lake; its area has added the cells in the merged lake. Due to the lack of high-resolution satellite imagery from 2013, it is impossible to determine whether the channel connecting the two lakes has existed in 2013.



0 0.15 0.3 0.6 Kilometers

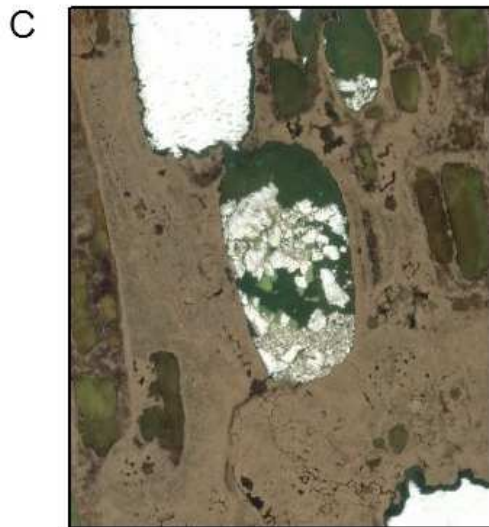
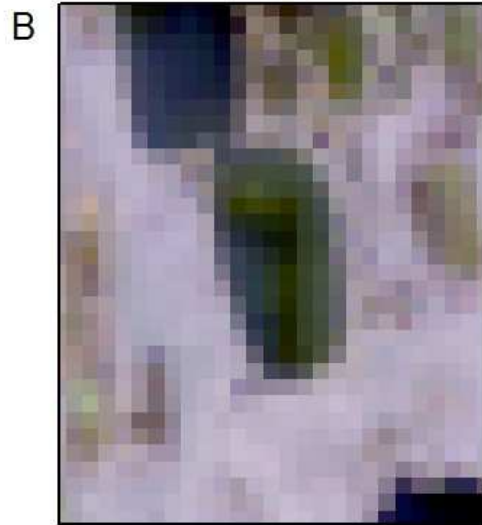
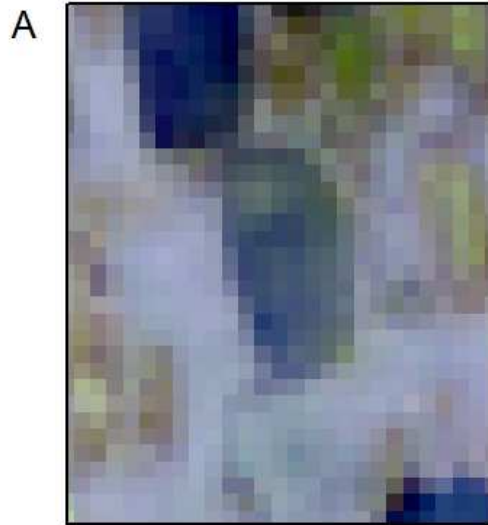


Figure 27. Example of a significantly grown lake; A – 2013, B – 2020, C – high resolution 2020.

6 Discussion

There are patterns seen in the distribution of the thaw lakes in the study area. The cumulative area of open water throughout the study area has grown during the study period from 2013 to 2020, even though the number of individual lakes decreases. Lake distribution depends on the surface elevation and ground ice content: the amount of lakes increases with ground ice content and decreases with elevation. Smaller lakes are more prevalent than large ones. However, there might be additional reasons for the distribution of the thaw lakes on the Arctic Coastal Plain.

6.1 Ground ice content

The study area is underlain by two types of permafrost, as seen in Fig. 28. The study area's major part is underlain by continuous permafrost with high excessive ground ice content (>20%) and high overburden (type CHF). In contrast, the southeastern quarter of the study area is underlain by continuous permafrost with low excessive ground ice content (<10%) and thin overburden (type CLF). The bedrock may be exposed in that site because the ground elevation slightly rises (see Fig. 11). To the south of the Alaskan Coastal Plain, the Brooks mountain ridge is located.

Lakes are depicted with dots placed at their polygon centroids. There are fewer lakes in the southeastern quarter, as seen in the figure. That is understandable because lake formation requires plenty of ground ice, which is only prominent in high ground ice content areas. By 2020, 224 lakes were located in the area of the type CLF permafrost, giving it the lake distribution density of 3.32 lakes/km². The remaining 2563 lakes are located in the type CHF permafrost area, giving it the lake distribution density of 5.62 lakes/km².

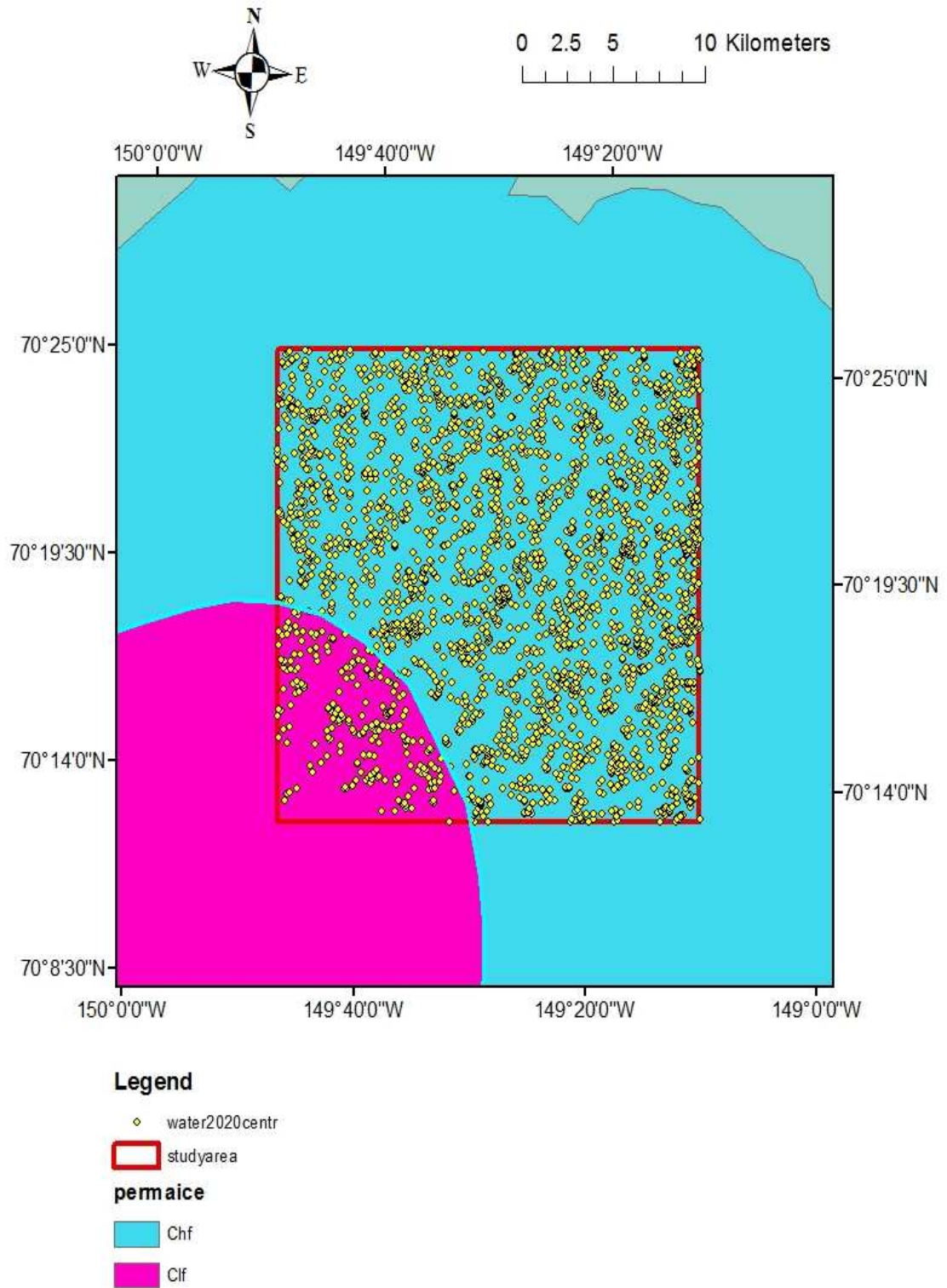
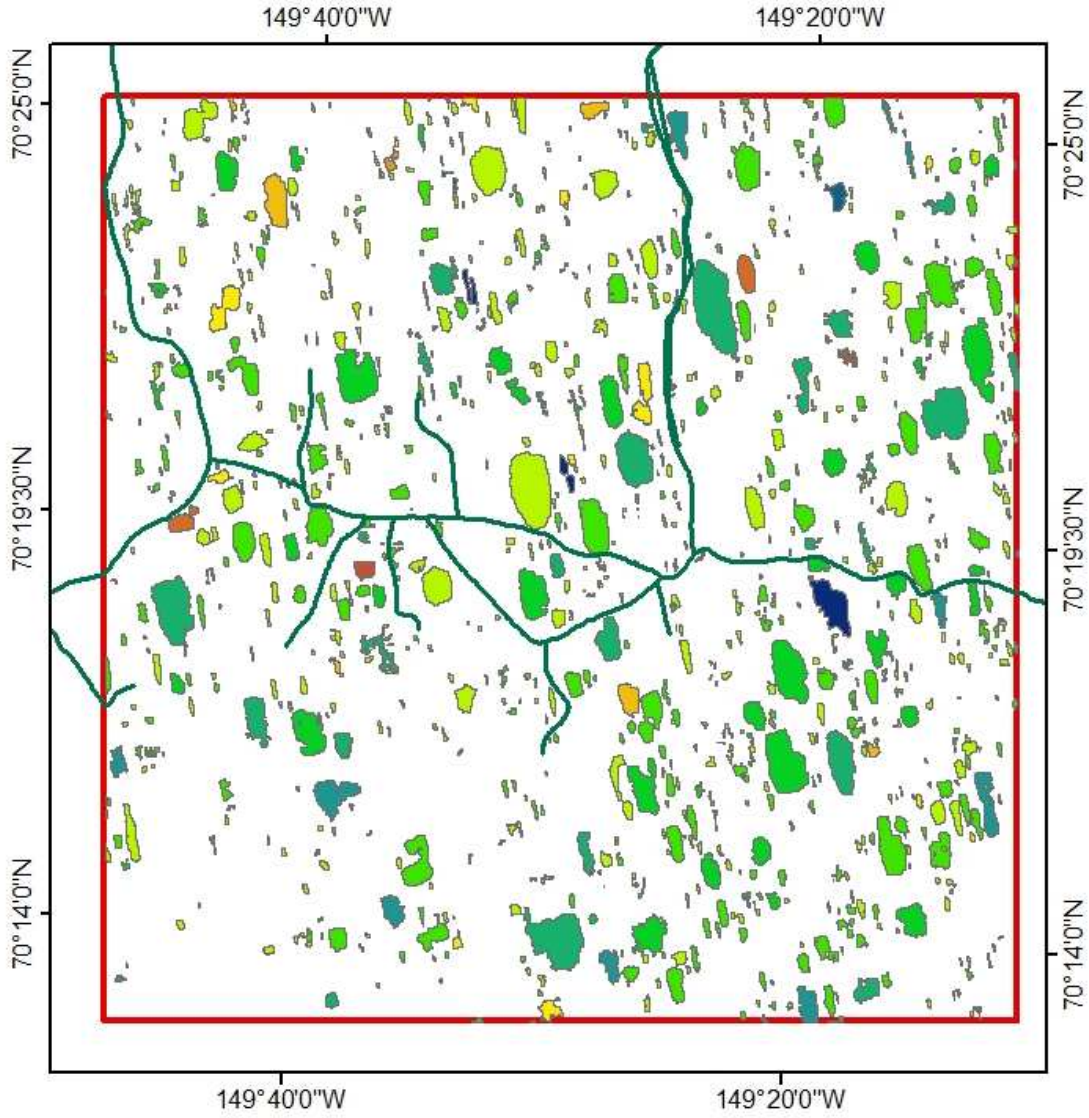


Figure 28. Permafrost types in the study area (data sourced from Brown et al, 2002)

6.2 Influence of infrastructure

As traffic in Alaska is restricted to designated routes in order to preserve the fragile tundra terrain and protect the underlying permafrost from thaw, the road network is not dense in the area. Figure 30 depicts the road network in the area; most of the roads belong to the petroleum industry. The roads in Alaska are built on artificial elevated berms for better stability, and they interfere with the local surface water drainage network. Therefore, natural water pathways are blocked, and water exchange in the area is interrupted or rerouted through culverts. That may cause unnatural accumulation of water in certain areas, if natural drainage from that location is blocked by a road. However, as seen from Figure 29, the lakes larger than 0.5 ha are distributed without the regard to the road network. It may mean that the road network has not interrupted the water drainage pathways in the first place; new pathways may have formed after the construction of the roads. To confirm the hypothesis, detailed observation of lakes adjacent to the road network is required.



Legend

— roads

▭ studyarea

Pixel count difference

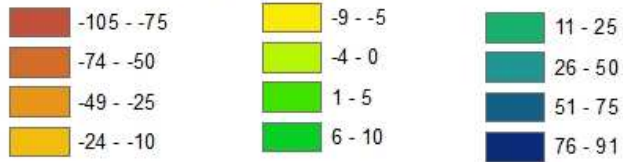


Figure 29. Roads in the study area (data sourced from State of Alaska Open Geodata Portal, 2019).

6.3 Precipitation

The mean annual precipitation in Deadhorse, Alaska is relatively low - 10 cm/yr (NOAA, 2011), which is normal for the subpolar climatic belt. Most of the precipitation falls in winter as snow between September and May, and in summer (June-August) there is rainfall.

The satellite images used for this research were acquired on 8 July 2013 and 01 August 2020. In 2013, the precipitation that might have had affected the lakes, was occurring from September 2012 to May 2013 as snow, and then in June as rainfall. There has fallen 1.72 inches (4.36 cm) of snow and 0.7 inches (1.8 cm) of rainfall. In 2019-2020, there was no precipitation detected at the Deadhorse Lake measuring station of the National Weather Service (2021) between September 2019 and July 2020. It appears that the measurements were not conducted at the station in that period. The comparison is impossible to make.

7 Conclusion

The presented research has shown that the area of open water in the study area has increased by 1.67% over the study period from 2013 to 2020. There are 2738 lakes in the area, of which 1092 have the area above 5000 m². Out of these large lakes, 566 lakes have grown over the study period with the annual rate of 435 m² per lake; The total number of lakes has reduced by 46 lakes (1.62%) during the study period. The lakes occupied 14.4% of the total study area in 2020, which is 0.3% more than in 2013.

Thaw lakes in the area are distributed according to the surface elevation and ground ice content; in the area of low ground ice content, the lake distribution density is 2.2 lakes/km² less than in the areas with high ground ice content.

Many lakes in the area have been detected to have huge changes in area over the study period; however, in some cases the huge area changes were caused by merging of multiple lakes, giving each lake the increase in area the size of added lakes. It is seen from this research that, although it is possible to draw a generalized conclusion that the lakes in the study area are growing in size, the exact reasons for the growth might be different in each lake.

The proposed method of open water detection in the Arctic tundra via NDWI has proven to be useful for this specific application; however, there are limitations to the method. Due to the lack of high-resolution materials, the current research was performed on the satellite images from Landsat-8, which have spatial resolution of 30 m. If the resolution of used images is higher, the detection's precision is expected to increase. Further development of this research would be the application of this method to satellite images with higher resolution.

It is advised that the NDWI detection method used in this research is applied for primary detection of open water areas; then, the results are recommended to be backed up by visual observation of possible artificial causes of area change, such as the merging of multiple lakes, or a drainage channel. If such apparent causes are not present in the immediate vicinity of a lake, then the changes in its area may be attributed to the degradation of permafrost in the lake's banks. The described approach to sorting out the values of area change not conforming with the general trend for the given area is seen to be useful for making general conclusions about the lake area dynamics and their distribution over the whole area.

Petroleum engineering in the Arctic is in substantial international demand; however, it is challenging because the infrastructure needs to interact with the underlying permafrost. Permafrost-associated hazards – thaw-freeze heave, thaw lakes, and slope instability – lead to deformation and destruction of petroleum infrastructure, jeopardizing performance. Emergency accidents result in costly repair and potential human losses.

Careful assessment of permafrost-related hazards is essential for geological and geotechnical investigation in the Arctic.

Studying permafrost is difficult because the region is remote, therefore, uninhabited; expeditions are dangerous and costly. This work focuses on evaluating the rate of permafrost degradation by studying geomorphologic features on the surface via remote sensing. Even though studying subsurface permafrost via remote sensing has its limitations, such as the inability to directly see the object of research (because it is underground), secondary signs of permafrost dynamics can be seen on the surface. Information inferred from these secondary signs is challenging to analyze (e.g., thaw lakes tend to increase in size due to the thawing of surrounding permafrost and decrease when new drainage channels are formed within thawing ground). However, remote sensing of secondary permafrost landscape features has proved itself to be reliable in engineering cryogeology.

8 Reference List

- Addison, P. E., Lautala, P., Oommen, T., & Vallos, Z. (2016). Embankment stabilization techniques for railroads on permafrost. In 2016 Joint Rail Conference. American Society of Mechanical Engineers Digital Collection.
- Addison, P., Baeckeroot, J., Oommen, T., Lautala, P., Koff, K., & Vallos, Z. (2015). Rail embankment investigation using remote sensing for a permafrost region. In *Cold Regions Engineering 2015* (pp. 90-101).
- Addison, P., Lautala, P. T., & Oommen, T. (2016). Utilizing vegetation indices as a proxy to characterize the stability of a railway embankment in a permafrost region. *AIMS Geosciences*, 2(4), 329.
- Alaska Mapping Executive Committee (2020). Alaska High Resolution Imagery (50cm). GeoNorth OIM AlaskaHighResolutionImagery CubeSERV, https://gis.dnr.alaska.gov/terrapixel/cubeserv/OIM_AlaskaHighResolutionImagery
- Alaskan Department of Fish and Game (n.a). Permafrost. ADFG website, <https://www.adfg.alaska.gov/index.cfm?adfg=ecosystems.permafrost#:~:text=If%20you%20dig%20down%20through,area%20is%20underlain%20by%20permafrost.>
- Alfred-Wegener Institut. (2019) Permafrost Modelling. AWI.de <https://www.awi.de/en/science/geosciences/permafrost-research/research-focus/permafrost-modelling.html>
- Alyeska Pipeline Service Group (APSG), (2017). Pump Station 1: the gateway to TAPS. Alyeska-pipe.com, Media Resources: Fact sheets, May 2017. https://www.alyeska-pipe.com/assets/uploads/pagestructure/NewsCenter_MediaResources_FactSheets_Entries/636307988497514156_2017FinalReducedSize.pdf
- AMAP, (2019). AMAP Climate Change Update 2019: An Update to Key Findings of Snow, Water, Ice and Permafrost in the Arctic (SWIPA) 2017. *Arctic Monitoring and Assessment Programme (AMAP), Oslo, Norway. 12 pp.*
- ArcGIS.com (2020). ArcMap Documentation. <https://desktop.arcgis.com/en/arcmap/>
- Arctic Centre (n.d.) definitions of the Arctic region. University of Lapland's Arctic Centre, <https://www.arcticcentre.org/EN/arcticregion/Maps/definitions>
- Arctic.ru (n.d.) Population. The Arctic, <https://arctic.ru/population/>
- Arendt, J. (2012) Biological Rhythms During Residence in Polar Regions, *Chronobiology International*, 29:4, 379-394, DOI: [10.3109/07420528.2012.668997](https://doi.org/10.3109/07420528.2012.668997)

- Bartsch, A. (2014). Requirements for Monitoring of Permafrost in Polar Regions. Requirements for Polar Permafrost Monitoring – Recommendations to the WMO-PSTG; Austran Polar Research Institute, Vienna, Austria.
- Belikovich, A.V. (2001). Vegetation of the northern part of Koryak Grange. *Vladivostok, Dalnauka Publishing*,. 420 p
- Black, Robert F., Barksdale, William L. (1949) Oriented Lakes of Northern Alaska. *The Journal of Geology* 1949 57:2, 105-118
- Brewer, M. C. (1958), The thermal regime of an Arctic lake, *Eos Trans. AGU*, 39(2), 278– 284, doi:10.1029/TR039i002p00278.
- Brown, J., Ferrians, O., Heginbottom, J. A., Melnikov, E. (2002). *Circum-Arctic Map of Permafrost and Ground-Ice Conditions, Version 2*. Boulder, Colorado USA. NSIDC: National Snow and Ice Data Center. doi: <https://doi.org/10.7265/skbg-kf16>.
- Cessna, A. (2009). The Arctic Circle. Universe Today, September 27, 2009, <https://www.universetoday.com/41636/the-arctic-circle/>
- Dobinski, W (2020). Permafrost active layer. *Earth-Science Reviews*, Volume 208, September 2020, 103301.
- Donev, J.M.K.C. et al. (2016). Energy Education - Permafrost [Online]. Available: <https://energyeducation.ca/encyclopedia/Permafrost>.
- Dunbar, M. (1973). Commentary: Stability and Fragility in Arctic Ecosystems. *Arctic*, 26(3), 179-185. Retrieved January 29, 2021, from <http://www.jstor.org/stable/40508439>
- Eppelbaum, L. V., Kutasov, I. M. (2019). Well drilling in permafrost regions: dynamics of the thawed zone. *Polar Research*, 38. <https://doi.org/10.33265/polar.v38.3351>
- Etzelmüller, B., Ødegård, R., Berthling, I., Sollid, J. (2001). Terrain parameters and remote sensing data in the analysis of permafrost distribution and periglacial processes: principles and examples from southern Norway. *Permafrost and Periglacial Processes*, 12(1), 79–92. <https://doi.org/10.1002/ppp.384>
- Frohn, R.C, Hinkel, K.M., Eisner, W.R. (2005) Satellite remote sensing classification of thaw lakes and drained thaw lake basins on the North Slope of Alaska. *Remote Sensing of Environment* 97 (2005) 116– 126
- Gao, B.C. (1996) NDWI—A normalized difference water index for remote sensing of vegetation liquid water from space. *Remote Sensing of Environment*, Volume 58, Issue 3, 1996, Pages 257-266, ISSN 0034-4257, [https://doi.org/10.1016/S0034-4257\(96\)00067-3](https://doi.org/10.1016/S0034-4257(96)00067-3). (<http://www.sciencedirect.com/science/article/pii/S0034425796000673>)

Gavrilov, A.A. (2014). Faults of the South Primorye as zone of geodynamic risk (according to the data of geologic and geomorphologic investigation of shores in the Peter the Great Bay). *Digest of V.I. Il'ichev Pacific Oceanological Institute, FEB RAS, Vladivostok, vol. 4.*

Gstaiger, V., Tian, J., Kiefl, R., Kurz, F. (2018) 2D vs. 3D Change Detection Using Aerial Imagery to Support Crisis Management of Large-Scale Events. *Remote Sens.* **2018**, 10(12), 2054; <https://doi.org/10.3390/rs10122054>

Hinkel, K M. Jones, B. M., Eisner, W. R., Cuomo, C. J., Beck, R A., Frohn, R. (2007) Methods to assess natural and anthropogenic thaw lake drainage on the western Arctic coastal plain of northern Alaska. *JOURNAL OF GEOPHYSICAL RESEARCH*, VOL. 112, F02S16, doi:10.1029/2006JF000584, 2007

Hinkel, K. (2006), Comment on ‘‘Formation of oriented thaw lakes by thaw slumping’’ by Jon D. Pelletier, *J. Geophys. Res.*, 111, F01021, doi:10.1029/2005JF000377.

Hinkel, K. M., Eisner, W. R., Bockheim, J. G., Nelson, F. E., Peterson, K. M., Dai, X. (2003) Spatial Extent, Age, and Carbon Stocks in Drained Thaw Lake Basins on the Barrow Peninsula, Alaska. *Arctic, Antarctic, and Alpine Research*, 35:3, 291-300, DOI: 10.1657/1523-0430(2003)035[0291:SEAACS]2.0.CO;2

Hinkel, K. M., Frohn, R. C., Nelson, F. E., Eisner, W. R., Beck, R. A. (2005) Morphometric and Spatial Analysis of Thaw Lakes and Drained Thaw Lake Basins in the Western Arctic Coastal Plain, Alaska. *PERMAFROST AND PERIGLACIAL PROCESSES*. *Permafrost and Periglac. Process.* 16: 327–341 (2005).

Hinkel, K.M., Eisner, W.R., Kim, C.J. (2017) Detection of tundra trail damage near Barrow, Alaska using remote imagery. *Geomorphology* 293 (2017) 360–367

Hinkel, K.M., Hurd, J.K. (2006). Permafrost Destabilization and Thaw following Snow Fence Installation, Barrow, Alaska, U.S.A. *Arctic, Antarctic, and Alpine Research*, Vol. 38, No. 4, 2006, pp. 530–539.

Hinkel, K.M., Jones, B. M., Eisner, W. R., Cuomo, C. J., Beck, R. A., Frohn, R. (2007). Methods to assess natural and anthropogenic thaw lake drainage on the western Arctic coastal plain of northern Alaska. *JOURNAL OF GEOPHYSICAL RESEARCH*, VOL. 112, F02S16, doi:10.1029/2006JF000584, 2007

Hinkel, K.M., Nelson, F.E. (2007) Anthropogenic heat island at Barrow, Alaska, during winter: 2001–2005. *JOURNAL OF GEOPHYSICAL RESEARCH*, VOL. 112, D06118, doi:10.1029/2006JD007837, 2007

Hughes, W., (n.d.) Challenges to arctic construction. AMConsultants.com
<https://amconsultants.com/experience/challenges-arctic-construction/>

IISD, (2019). Arctic States Reaffirm Commitment to Sustainable Development of Arctic Ecosystems and People. *International Institute of Sustainable Development, SDG Knowledge Hub*, <https://sdg.iisd.org/news/arctic-states-reaffirm-commitment-to-sustainable-development-of-arctic-ecosystems-and-people/>

Instones, A., Anisimov, O. (2016) Climate Change and Arctic Infrastructure; Proceedings of the 9th International Conference on Permafrost (NICOP), Fairbanks, Alaska, USA, June 29-July 3, 2008, pp. 779-784.

Jones, B. M., Arp, C. D. (2009) Arctic Lake Physical Processes and Regimes with Implications for Winter Water Availability and Management in the National Petroleum Reserve Alaska. *Environmental Management (2009) 43:1071–1084*

Jones, B. M., Arp, C. D. (2009) Arctic Lake Physical Processes and Regimes with Implications for Winter Water Availability and Management in the National Petroleum Reserve Alaska. *Environmental Management (2009) 43:1071–1084*

Jorgenson, M. T., Grosse, G. (2016). Remote Sensing of Landscape Change in Permafrost Regions. *PERMAFROST AND PERIGLACIAL PROCESSES*, Permafrost and Periglac. Process. 27: 324–338 (2016)

Kääb, A. (2008). Review of Remote sensing of permafrost-related problems and hazards. *Permafrost and Periglacial Processes*, 19(2), 107–136. <https://doi.org/10.1002/ppp.619>

Karjalainen, O., Aalto, J., Luoto, M. *et al.* (2019) Circumpolar permafrost maps and geohazard indices for near-future infrastructure risk assessments. *Sci Data* 6, 190037 (2019). <https://doi.org/10.1038/sdata.2019.37>

Lantz, Trevor. (2017). Vegetation Succession and Environmental Conditions following Catastrophic Lake Drainage in Old Crow Flats, Yukon. *ARCTIC*. 70. 177. [10.14430/arctic4646](https://doi.org/10.14430/arctic4646).

Larsen, J.N, Fondahl, G. (2015). Arctic Human Development Report: Regional Processes and Global Linkages. Copenhagen: Nordisk Ministerråd, 2015., p. 500

Lecavalier, B., Fisher, D. A., Milne, G.A., *et al.* (2017). Arctic temperatures and Greenland evolution. *Proceedings of the National Academy of Sciences* Jun 2017, 114 (23) 5952-5957; DOI: 10.1073/pnas.1616287114

Mackay, J. R. (1992) Lake stability in ice-rich permafrost environment: examples from the Eastern Arctic Coast. *NHRI Symposium Series 7, Environment Canada, Saskatoon, 1992*.

Malneva, I. V., Krestin, B.M., Kononova, N. K., (2016). Hazard assessment of geological engineering processes in the catchment of the Amur river. *Materials of XVIII Conference*

on fundamental problems and applications of engineering geology and geoecology, EGI RAS, pp. 158 - 163.

Manoli, G., Fatichi, S., Schläpfer, M. (2019) Magnitude of urban heat islands largely explained by climate and population. *Nature* 573, 55–60 (2019).
<https://doi.org/10.1038/s41586-019-1512-9>

Mars, J.C., Houseknecht, D.W. (2007) Quantitative remote sensing study indicates doubling of coastal erosion rate in past 50 yr along a segment of the Arctic coast of Alaska. *Geology*; July 2007, no. 7; p. 583–586; doi: 10.1130/G23672A

McFeeters, S. (1996). The use of the Normalized Difference Water Index (NDWI) in the delineation of open water features. *International Journal of Remote Sensing*, 17(7), 1425–1432. <https://doi.org/10.1080/01431169608948714>

Mondejar, J.P., Tongco, A.F. (2019) Near infrared band of Landsat 8 as water index: a case study around Cordova and Lapu-Lapu City, Cebu, Philippines. *Sustain Environ Res* 29, 16 (2019). <https://doi.org/10.1186/s42834-019-0016-5>

Monroe, R. (2020). RESEARCHERS FIND NEW REASON WHY ARCTIC IS WARMING SO FAST. UC San Diego Scripps Institute of Oceanography.
<https://scripps.ucsd.edu/news/researchers-find-new-reason-why-arctic-warming-so-fast>

NASA Earth Observatory, (n.d.). Tundra: Mission: Biomes.
<https://earthobservatory.nasa.gov/biome/biotundra.php#:~:text=Description,Europe%2C%20and%20Siberia%20in%20Asia.>

NASA.gov (2013). Landsat 8 Overview. NASA Landsat Science,
<https://landsat.gsfc.nasa.gov/landsat-8/landsat-8-overview>

National Oceanic & Atmospheric Administration (NOAA) (2011). Summary of Annual Normals 1981-2010. National Environmental Satellite, Data, and Information Service, Station: DEADHORSE AIRPORT, AK US USW00027406.

National Park Service (n.d.). Wildlife of the Arctic. *NPS.gov*,
<https://www.nps.gov/subjects/arctic/wildlife.htm>

National Park Service (NPS.gov), (2018). Tundra. Lake Clark National Park and Preserve, Alaska.
<https://www.nps.gov/lacl/learn/nature/tundra.htm#:~:text=There%20are%20two%20kind%20of,north%20of%20the%20arctic%20circle.&text=Even%20once%20the%20snow%20has,where%20only%20the%20heartiest%20survive.>

National Research Council. 1995. Wetlands: Characteristics and Boundaries. Washington, DC: The National Academies Press. <https://doi.org/10.17226/4766>.

- National Snow and Ice Data Center (2020). *All About Arctic Climatology and Meteorology*. <https://nsidc.org/cryosphere/arctic-meteorology/>.
- National Snow and Ice Data Center (NSIDC) (2017). State of the Cryosphere: Permafrost and Frozen Ground. <https://nsidc.org/cryosphere/sotc/permafrost.html>
- National Weather Service (2020). Alaska snow data (archives). Weather.gov, https://www.weather.gov/aprfc/Snow_Depth#
- Nationsonline.org (n.d.). Map of Alaska. US State Maps, Nations Online, https://www.nationsonline.org/oneworld/map/USA/alaska_map.htm
- Nguyen, T., Burn, C., King, D., Smith, S. (2009). Estimating the extent of near-surface permafrost using remote sensing, Mackenzie Delta, Northwest Territories. *Permafrost and Periglacial Processes*, 20(2), 141–153. <https://doi.org/10.1002/ppp.637>
- Niiler, E. (2019). The Arctic Is Warming Much Faster Than the Rest of Earth. *Wired.com* <https://www.wired.com/story/the-arctic-is-warming-much-faster-than-the-rest-of-earth/>
- Okhlopkova, T.V., Guryanov, G.R., Plotnikov, A.A. (2018). Building and construction on permafrost. *Don Engineering Digest*, no. 4 (51), 2018, pp. 184.
- Osborne, E., Richter-Menge, J., Jeffries, M. (2018). 2018 Arctic Report Card: Executive summary. NOAA's Arctic Program, <https://www.arctic.noaa.gov/Report-Card/Report-Card-2018/ArtMID/7878/ArticleID/772/Executive-Summary>
- Palinkas, L.A, Suedfeld, P. (2008) Psychological effects of polar expeditions. *Lancet*. 2008 Jan 12;371(9607):153-63. doi: 10.1016/S0140-6736(07)61056-3. PMID: 17655924.
- Planet.com (2020). Explorer (portal), https://www.planet.com/explorer/#/mosaic/431b62a0-eaf9-45e7-acf1-d58278176d52.global_monthly_2021_01_mosaic/zoom/2.48 (accessed 01 Jan 2021)
- Post, E, Alley, R. B., Christensen, T. R (2019). The polar regions in a 2°C warmer world. *Science Advances* 04 Dec 2019: Vol. 5, no. 12, DOI: 10.1126/sciadv.aaw9883
- Roy, D.P. ,Kovalskyy, V., Zhanga, H.K., Vermote, E.F., Yan, L., Kumar, S.S., Egorova, A. (2016). Characterization of Landsat-7 to Landsat-8 reflective wavelength and normalized difference vegetation index continuity. *Remote Sensing of Environment*
- Saito, H.; Iijima, Y.; Basharin, N.I.; Fedorov, A.N.; Kunitsky, V.V., (2018) Thaw Development Detected from High-Definition Topographic Data in Central Yakutia. *Remote Sens.* **2018**, *10*, 1579. <https://doi.org/10.3390/rs10101579>
- Schollaen, K, Gonçalo V, Lewkowicz, A (2014) “Report from the International Permafrost Association: Fourth European Conference on Permafrost (EUCOP4): Report

from the International Permafrost Association. Permafrost and periglacial processes 25.4 (2014): 344–348. Web.

Schuur, T (2019). Permafrost and the Global Carbon Cycle. Center for Ecosystem Science and Society, Northern Arizona University, Flagstaff, AZ, USA.

Schuur, T. (2019). Permafrost and the Global Carbon Cycle. Arctic Report Card: Update for 2019. The Arctic Program, <https://arctic.noaa.gov/Report-Card/Report-Card-2019/ArtMID/7916/ArticleID/844/Permafrost-and-the-Global-Carbon-Cycle>

Severpost.ru (2020). Polar bear killed a man in Spitsbergen. Severpost, 28 August 2020, <https://severpost.ru/read/100871/>

State of Alaska Open Geodata Portal (2019). Infrastructure. <https://gis.data.alaska.gov/datasets/infrastructure-map-service>

State of Alaska Open Geodata Portal (2020). Infrastructure Map Service, arcgis.dnr.alaska.gov.

State of Alaska, (n.d.). Facts about Alaska. *Alaska.gov*, <http://alaska.gov/kids/learn/facts.htm>

Sulikowska, A., Walawender, J.P., Walawender, E. (2019) Temperature extremes in Alaska: temporal variability and circulation background. *Theor Appl Climatol* 136, 955–970 (2019). <https://doi.org/10.1007/s00704-018-2528-z>

UN Environment (n.d.). Arctic Region. ONU Programme pour l'environnement. UNenvironment.org, <https://www.unenvironment.org/fr/node/958#:~:text=The%20Arctic%20is%20also%20characterized,of%20sea%2C%20snow%20and%20ice>.

United States Census Bureau (2018). Cartographic Boundary Files. Census.gov, <https://www.census.gov/geographies/mapping-files/time-series/geo/carto-boundary-file.html>

United States Geological Survey (USGS.gov), (2019). EarthExplorer Help Page, *USGS.com*, https://lta.cr.usgs.gov/EEHelp/ee_help

University of Edinburgh (2019). Can plants help to prevent permafrost thaw? Social Responsibility and Sustainability initiative, <https://www.ed.ac.uk/sustainability/what-we-do/climate-change/case-studies/climate-research/can-plants-prevent-permafrost-thaw>

US Museum of Paleontology (USMP), (n.d.) The tundra biome. The world's biomes, <https://ucmp.berkeley.edu/exhibits/biomes/tundra.php>

Volume 185, November 2016, Pages 57-70. https://doi.org/10.1016/j.rse.2015.12.024

Wagner, A.M., Lindsey, N.J., Dou, S, et al. (2018). Permafrost Degradation and Subsidence Observations during a Controlled Warming Experiment. *Sci Rep* 8, 10908 (2018). <https://doi.org/10.1038/s41598-018-29292-y>

Waldman, S (2017). Lightning-Caused Fires Rise in Arctic as the Region Warms. *Scientific America*, June 27, 2017, [scientificamerican.com](https://www.scientificamerican.com/article/lightning-caused-fires-rise-in-arctic-as-the-region-warms/)
<https://www.scientificamerican.com/article/lightning-caused-fires-rise-in-arctic-as-the-region-warms/>

Weatherspark.com (2021) Average weather at Deadhorse, Alaska.
<https://weatherspark.com/y/145086/Average-Weather-at-Deadhorse-Airport-Alaska-United-States-Year-Round#Sections-Precipitation>

Williams, A., O'Sullivan Darcy, A., Wilkinson, A. (2011). The future of Arctic enterprise: Long-term outlook and implications. *Smith School of Enterprise and the Environment, University of Oxford, November 2011*,
<https://www.smithschool.ox.ac.uk/publications/reports/ssee-arctic-forecasting-study-november-2011.pdf>

WWF (n.d.) Species: polar bear. *World Wildlife Fund*,
<https://www.worldwildlife.org/species/polar-bear>

Young, K, Chatwood, S, Rawat, R. (2010) Data brief from the Circumpolar Health Observatory. Introduction and population [2010-1], vol. 69, *International journal of circumpolar health*.